

Osteology of *Batrachuperus londongensis* (Urodela, Hynobiidae): study of bony anatomy of a facultatively neotenic salamander from Mount Emei, Sichuan Province, China (#21096)

1

First submission

Editor guidance

Please submit by **6 Nov 2017** for the benefit of the authors (and your \$200 publishing discount).



Structure and Criteria

Please read the 'Structure and Criteria' page for general guidance.



Raw data check

Review the raw data. Download from the [materials page](#).



Image check

Check that figures and images have not been inappropriately manipulated.

Privacy reminder: If uploading an annotated PDF, remove identifiable information to remain anonymous.

Files

Download and review all files from the [materials page](#).

11 Figure file(s)


1 Table file(s)



Structure your review

The review form is divided into 5 sections.
Please consider these when composing your review:

1. BASIC REPORTING
2. EXPERIMENTAL DESIGN
3. VALIDITY OF THE FINDINGS
4. General comments
5. Confidential notes to the editor






 You can also annotate this PDF and upload it as part of your review

When ready [submit online](#).





Editorial Criteria

Use these criteria points to structure your review. The full detailed editorial criteria is on your [guidance page](#).





BASIC REPORTING

-  Clear, unambiguous, professional English language used throughout.
-  Intro & background to show context. Literature well referenced & relevant.
-  Structure conforms to [PeerJ standards](#), discipline norm, or improved for clarity.
-  Figures are relevant, high quality, well labelled & described.
-  Raw data supplied (see [PeerJ policy](#)).

EXPERIMENTAL DESIGN

-  Original primary research within [Scope of the journal](#).
-  Research question well defined, relevant & meaningful. It is stated how the research fills an identified knowledge gap.
-  Rigorous investigation performed to a high technical & ethical standard.
-  Methods described with sufficient detail & information to replicate.

VALIDITY OF THE FINDINGS

-  Impact and novelty not assessed. Negative/inconclusive results accepted. *Meaningful* replication encouraged where rationale & benefit to literature is clearly stated.
-  Data is robust, statistically sound, & controlled.
-  Conclusions are well stated, linked to original research question & limited to supporting results.
-  Speculation is welcome, but should be identified as such.

Standout reviewing tips

3



The best reviewers use these techniques

Tip

Support criticisms with evidence from the text or from other sources

Example

Smith et al (J of Methodology, 2005, V3, pp 123) have shown that the analysis you use in Lines 241-250 is not the most appropriate for this situation. Please explain why you used this method.

Give specific suggestions on how to improve the manuscript

Your introduction needs more detail. I suggest that you improve the description at lines 57- 86 to provide more justification for your study (specifically, you should expand upon the knowledge gap being filled).

Comment on language and grammar issues

The English language should be improved to ensure that an international audience can clearly understand your text. Some examples where the language could be improved include lines 23, 77, 121, 128 – the current phrasing makes comprehension difficult.

Organize by importance of the issues, and number your points

1. Your most important issue
2. The next most important item
3. ...
4. The least important points

Please provide constructive criticism, and avoid personal opinions

I thank you for providing the raw data, however your supplemental files need more descriptive metadata identifiers to be useful to future readers. Although your results are compelling, the data analysis should be improved in the following ways: AA, BB, CC

Comment on strengths (as well as weaknesses) of the manuscript

I commend the authors for their extensive data set, compiled over many years of detailed fieldwork. In addition, the manuscript is clearly written in professional, unambiguous language. If there is a weakness, it is in the statistical analysis (as I have noted above) which should be improved upon before Acceptance.

Osteology of *Batrachuperus londongensis* (Urodela, Hynobiidae): study of bony anatomy of a facultatively neotenic salamander from Mount Emei, Sichuan Province, China

Jian-ping Jiang¹, Jia Jia², Meihua Zhang¹, Ke-Qin Gao^{Corresp. 2}

¹ Chengdu Institute of Biology, Chinese Academy of Sciences, Chengdu, China

² School of Earth and Space Sciences, Peking University, Beijing, China

Corresponding Author: Ke-Qin Gao

Email address: kqgao@pku.edu.cn

The Longdong Stream Salamander *Batrachuperus londongensis*, living in a mountain stream environment at Mt. Emei in Sichuan Province, China, represents a rare species that is facultatively neotenic in the family Hynobiidae. Although the species has been known to science for some 40 years since its initial discovery in the late 1970s, anatomical details of its osteology remain poorly understood and developmental information is still lacking for the species. This study 1) provides a detailed osteological account of *Batrachuperus londongensis* based on micro-CT scanning and clearing and staining of multiple specimens from the type locality; 2) provides a discussion of intraspecific variation related to life-history differences; and 3) presents a discussion on limb features related to morphological evolution of limb patterns correlative with ecological adaptation to mountain stream environments. Osteological comparisons with congeneric species has led to recognition of several diagnostic features that are unique to *B. londongensis*, including: vomers widely separated from one another, lacking a midline contact; presence of uncommon perichondral ossification of the ascending process of the palatoquadrate as part of the suspensorium; and presence of a prominent posterodorsal process of the scapular blade for ligamentous insertion of the levator muscle of the scapula. In addition, some but not all neotenic individuals retain the palatine as a discrete element, indicative of its delayed absorption after sexual maturity. Postmetamorphic and neotenic individuals are strikingly different in the complexity of hyobranchial structures. Neotenes display a high degree of ossification of hyobranchial elements, tend to increase ossification of both hypobranchial I and ceratobranchial I during aging, and retain fully ossified ceratobranchial III and IV; in contrast, these elements remain entirely cartilaginous or are totally lost by resorption in postmetamorphic individuals. In addition, all postmetamorphic forms display an inverted “T”-shaped basibranchial II, whereas neotenes show transformation from a “fork”-shaped

to the “T”-shaped configuration after sexual maturity. *Batrachuperus londongensis* displays a mosaic of apomorphic and plesiomorphic states in its limb ossifications: presence of a single centrale element in both the manus and pes is a derived condition in Hynobiidae and other families as well, whereas retention of a postminimus in the pes is obviously plesiomorphic within Urodela. Reduction in number of digits from five to four in the pes and possession of a cornified sheath covering the terminal phalanges are also derived features shared with some but not all mountain stream salamanders that are adapted to a similar type of environment.

**Osteology of *Batrachuperus londongensis* (Urodela,
Hynobiidae): study of bony anatomy of a facultatively
neotenic salamander from Mount Emei, Sichuan Province,
China**

Jian-ping Jiang¹, Jia Jia², Meihua Zhang¹, Ke-Qin Gao²

¹Chengdu Institute of Biology, Chinese Academy of Sciences, Chengdu 610041, China

²School of Earth and Space Sciences, Peking University, Beijing 100871, China

Corresponding authors: Ke-Qin Gao, 5 Yiheyuan Road, Beijing 100871, China

Email address: kqgao@pku.edu.cn

16

17 Abstract

18 The Longdong Stream Salamander *Batrachuperus londongensis*, living in a mountain stream
 19 environment at Mt. Emei in Sichuan Province, China, represents a rare species that is
 20 facultatively neotenic in the family Hynobiidae. Although the species has been known to science
 21 for some 40 years since its initial discovery in the late 1970s, anatomical details of its osteology
 22 remain poorly understood and developmental information is still lacking for the species. This
 23 study 1) provides a detailed osteological account of *Batrachuperus londongensis* based on micro-
 24 CT scanning and clearing and staining of multiple specimens from the type locality; 2) provides
 25 a discussion of intraspecific variation related to life-history differences; and 3) presents a
 26 discussion on limb features related to morphological evolution of limb patterns correlative with
 27 ecological adaptation to mountain stream environments. Osteological comparisons with
 28 congeneric species has led to recognition of several diagnostic features that are unique to *B.*
 29 *londongensis*, including: vomers widely separated from one another, lacking a midline contact;
 30 presence of uncommon perichondral ossification of the ascending process of the palatoquadrate
 31 as part of the suspensorium; and presence of a prominent posterodorsal process of the scapular
 32 blade for ligamentous insertion of the levator muscle of the scapula. In addition, some but not all
 33 neotenic individuals retain the palatine as a discrete element, indicative of its delayed absorption
 34 after sexual maturity. Postmetamorphic and neotenic individuals are strikingly different in the
 35 complexity of hyobranchial structures. Neotenes display a high degree of ossification of
 36 hyobranchial elements, tend to increase ossification of both hypobranchial I and ceratobranchial
 37 I during aging, and retain fully ossified ceratobranchial III and IV; in contrast, these elements
 38 remain entirely cartilaginous or are totally lost by resorption in postmetamorphic individuals. In

addition, all postmetamorphic forms display an inverted “T”-shaped basibranchial II, whereas neotenes show transformation from a “fork”-shaped to the “T”-shaped configuration after sexual maturity. *Batrachuperus londongensis* displays a mosaic of apomorphic and plesiomorphic states in its limb ossifications: presence of a single centrale element in both the manus and pes is a derived condition in Hynobiidae and other families as well, whereas retention of a postminimus in the pes is obviously plesiomorphic within Urodela. Reduction in number of digits from five to four in the pes and possession of a cornified sheath covering the terminal phalanges are also derived features shared with some but not all mountain stream salamanders that are adapted to a similar type of environment.

Subjects Zoology, Evolutionary Studies, Taxonomy

Keywords *Batrachuperus londongensis*, Hynobiid salamander, Facultative neoteny, Osteology, Character evolution

Introduction

The family Hynobiidae consists of 66–67 species in 9–11 genera (Fei et al., 2006; AmphibiaWeb, 2017; Frost, 2017). These are small to medium sized salamanders found primarily in Asia, although geographical range of one species (the Siberian salamander *Salamandrella keyserlingii*) extends from Asia into European Russia (AmphibiaWeb, 2017; Frost, 2017). Phylogenetically, the Hynobiidae form the sister clade with Cryptobranchidae, the two families together classified in the suborder Cryptobranchoidea Dunn, 1922. The Hynobiidae have long been viewed as a group of primitive salamanders, as they lack derived features such as

62 fusion of the angular with the prearticular in the lower jaw, but retain plesiomorphic features,
63 including external fertilization (Dunn, 1923; Noble, 1931), a large number of chromosomes ($2n=$
64 40–78), and the presence of microchromosomes (Morescalchi, 1973, 1975; Edwards, 1976;
65 Sessions, 2008).

66 Based on the fossil record from northern China, the evolutionary history of the
67 Hynobiidae can be traced back to Aptian time (~125 Ma) during the Early Cretaceous (Chen &
68 Gao, 2009; Gao, Chen & Jia, 2013; Jia & Gao, 2016b). Several fossil taxa from China including
69 *Liaoxitriton* and *Nuominerpeton* are apparently stem-group hynobiids, as evidenced by their
70 possession of derived features shared with extant hynobiids, including: transverse and arched
71 vomerine tooth rows; a deeply notched posterolateral border of the vomer for choana; and an
72 optic foramen opening at the notched posterior border of orbitosphenoid (Chen & Gao, 2009;
73 Gao, Chen & Jia, 2013; Jia & Gao, 2016a). Because *Liaoxitriton* and *Nuominerpeton* can be
74 readily recognized as hynobiid-like salamanders (Chen & Gao, 2009; Jia & Gao, 2016a), the
75 fossil record indicates that the split of the hynobiid from cryptobranchid clade seems to be a
76 phylogenetic event that had taken place no later than the Aptian time (~125 Ma). Recent
77 analyses of the nuclear exon and mitochondrial genome also estimate the time of origin of extant
78 hynobiids as roughly 125 Ma (Zheng et al., 2011). A more recent analysis of nuclear genes,
79 however, yielded an estimate of 135 Ma for the origin of crown-group hynobiids (Chen et al.,
80 2015), which is significantly older than the previous estimate of 125 Ma and the evidence from
81 the fossil record.

82 Most hynobiids are terrestrial in the adult stage, but species in several genera
83 (*Batrachuperus*, *Liua*, *Pachyhynobius*, *Ranodon* and *Paradactylodon*) are mostly mountain
84 stream dwellers that can be found in water all year around (Reilly, 1983; Fei et al., 2006;

Sparreboom, 2014; AmphibiaWeb, 2017). In terms of life-history features, most hynobiids have a biphasic life cycle, with a gilled aquatic larval stage going through metamorphosis to a postmetamorphic adult stage. The exception is the Japanese species *Hynobius retardatus*, which has been reported as partly neotenic as a population variant from Lake Kuttarush in Hokkaido, with some specimens reaching a total length of 150 mm while retaining gills (Sasaki, 1924). However, this population now appears to be extinct, with no osteological description of the population ever undertaken (Inukai, 1930–1932; Wakahara, 1996). Accordingly, *Batrachuperus londongensis* Liu & Tian, 1978, commonly known as the Longdong Stream Salamander, appears to be the only extant hynobiid species that has been documented as facultatively neotenic (Fei et al., 2006). Osteological study of this unusual hynobiid is bound to be significant for understanding patterns of ossification of the cranium and post-cranium, and for reconstruction of the evolution of hynobiid salamanders more generally. Furthermore, such an osteological study is in urgent need because the species in question is endangered (see below).

Within Hynobiidae, the genus *Batrachuperus* includes six or seven species (Fu & Zeng, 2008; Fei et al., 2006; Fei, Ye & Jiang, 2010) that are all endemic to western China. The genus consists of the type species *Batrachuperus pinchonii* (David, 1872) plus five other species (*B. londongensis*, *B. tibetanus*, *B. yenyuanensis*, *B. taibaiensis*, and *B. karlschmidtii*; see Fei et al., 2006; Fu & Zeng, 2008). Another nominal taxon, *Batrachuperus cochraniae* Liu, 1950, was synonymized with *Batrachuperus pinchonii* based on molecular evidence (Fu & Zeng, 2008), but the validity of the name is still in dispute (Fei, Ye & Jiang, 2010, 2012). All of these are aquatic forms that inhabit mountain stream and/or plateau pond environments, at elevations ranging from 1200 m–4400 m above sea level (Fei et al., 2006; Fei, Ye & Jiang, 2010). In terms of conservation status, most of these species are currently vulnerable (Jiang et al., 2016). Two

species known from Iran (“*Batrachuperus*” *persicus*; see AmphibaWeb, 2017 for status of “*Batrachuperus*” *gorganensis*) and one from Afghanistan (“*Batrachuperus*” *mustersi*) were previously classified in *Batrachuperus*, but now are treated as species in *Paradactylodon* (see AmphibiaWeb, 2017 for comments); based on molecular evidence, these are probably more closely related to *Ranodon* than to other hynobiids (Zhang et al., 2006; Zheng et al., 2011; Weisrock et al., 2013; Chen et al., 2015;). No fossil record has been found for *Batrachuperus* or its sister clade (*Liua* + *Pseudohynobius*). Based on molecular data alone, *Batrachuperus* was estimated as having originated in the late Miocene (~7.3 Ma) in a recent analysis using 29 nuclear genes (Chen et al., 2015), a much younger date than the estimation of ~24.3 Ma based on the complete mitochondrial genome (Zhang et al., 2006) or that of 20–30 Ma based on complete mitochondrial genome and three nuclear genes (Zheng et al., 2011).

Batrachuperus is one of the several hynobiid genera (*Batrachuperus*, *Liua*, *Pachyhynobius*, *Paradactylodon*, *Pseudohynobius*) that have received little study of their developmental osteology (Rose, 2003); moreover, anatomical details remain poorly known for these taxa. For the genus *Batrachuperus*, brief osteological accounts of the type species, *Batrachuperus pinchonii* can be found in the literature (e.g., Zhang et al., 2009; Xiong et al., 2013a); however, adequate osteological description of *Batrachuperus londongensis* is still lacking, although the species has been known to science for almost 40 years since its discovery in the late 1970s. In regard to phylogenetic relationships, few adequate data can be found in the literature on osteological details of the species. Attempting to improve this awkward situation, our study provides a detailed osteological account of *Batrachuperus londongensis* and a morphological comparison in relation to life-history differences within this species; in addition, we present a discussion on diagnosis of the species based on bony features, patterns of

ossification of the hyobranchium and limb ossification. Phylogenetic analysis will be performed in future research when necessary data becomes available for other congeneric species.

Materials & Methods

A total of 12 specimens of *Batrachuperus londongensis* were used in this study, including both juveniles and adults, and both postmetamorphic and neotenic individuals (Table 1). The material used includes both dry skeletons and fluid-preserved (10% formaldehyde) specimens. In addition, cleared and stained specimens (CIB 14499, 14504) allowed observation of both bony and cartilaginous structures. All of these specimens are deposited in the Chengdu Institute of Biology (CIB), Chinese Academy of Sciences, Chengdu, China. For purpose of comparison, several specimens belonging to congeneric species were included in this study: FMNH 170703 (referred specimen of *B. pinchonii*), CIB 20040235 (referred specimen of *B. taibaiensis*), FMNH 49380 (paratype of *B. karlschmidtii*), FMNH 5901 (paratype of *B. tibetanus*), FMNH 49371 (paratype of *B. yenyuanensis*).

Total length (TL) refers to the measurement between the tip of the snout and the posterior extremity of the tail; snout–pelvic length (SPL) is the measurement from the tip of the snout to the posterior end of the pelvis (marked by the anus in fluid-preserved specimens and by the haemal arch of the last caudosacral in dry skeletons). Skull length (SKL) refers to the maximum dimension from the tip of the snout to the posterior end of the occipital condyles; skull width (SKW) is the distance measured between the cranio-mandibular joints. All measurements are in millimeters (mm). Anatomical nomenclatures follow Francis (1934), Reilly and Lauder (1988), and Shubin and Wake (2003), with the exceptions as noted in several cases.

The type specimen of *Batrachuperus londongensis* is a large male, with a TL of 265 mm

and a SPL of 129 mm (Fig. 1). The specimen carries a field number CIB 65I0013 as in previous publications (e.g., Fei, Ye & Tian, 1983; Fei et al., 2006), but it has been formally catalogued as CIB 65I0013/14380 in specimen collections at the Chengdu Institute of Biology (Fig. 1). This specimen represents a neotenic form as it retains gill slits and a larval type of hyobranchium (Fei, Ye & Tian, 1983; Fei et al., 2006). The specimen was collected on March 23, 1965 from the type locality, Longdong Stream at Mount Emei (Emeishan), at an elevation of 1300 m above sea level as has been documented in the literature (Liu & Tian, 1978; Fei, Ye & Tian, 1983). Subsequent collections of specimens were made in 2002, 2006, 2014 and 2016 from the same mountain stream by field crews from the Chengdu Institute of Biology.

Selected specimens from the CIB collections (Table 1), including the holotype (CIB 65I0013/14380), were CT scanned using a high-resolution X-ray scanner (Quantum GX micro-CT Imaging System, PerkinElmer®) at the Chengdu Institute of Biology, Chinese Academy of Sciences. These specimens were scanned along the coronal axis at an image resolution of 2000 X 2000. Comparative specimens from the FMNH collections were CT scanned at the University of Chicago (PaleoCT Lab) using a dual tube X-ray scanner from GE. Segmentation and three-dimensional reconstruction of the CT images were made by using VG Studio Max 2.2 (Volume Graphics, Heidelberg, Germany).

Two specimens (CIB 14504, 14499) were whole-mount cleared and double stained after being scanned. The clearing and staining procedures followed the protocols of Hanken & Wassersug (1981). Cartilaginous elements were stained in blue using Alcian Blue 8GX and bony structures were stained in red using Alizarin Red, and then were cleared in glycerin KOH solution. Line drawings of skeletal structures were prepared using Adobe Photoshop® CS6 software, and are presented as text figures and supplementary figures (Supporting Information).

177

178 **Institutional abbreviations**—**CIB**, Chengdu Institute of Biology, Chinese Academy of
179 Sciences, Chengdu, China; **FMNH**, Field Museum of Natural History, Chicago, USA; **MVZ**,
180 Museum of Vertebrate Zoology, University of California, Berkeley, USA.

181

182 **Anatomical abbreviations**—**act**, acetabulum; **adf**, anterodorsal fenestra; **amf**, anteromedial
183 fenestra; **an**, angular; **ar**, articular; **at**, atlas; **bb**, basibranchial; **bc**, basale commune; **c**, centrale;
184 **cb**, ceratobranchial; **ch**, ceratohyal; **corn**, cornua; **crd**, crista dorsalis; **crv**, crista ventralis; **den**,
185 dentary; **dc**, distal carpal; **dt**, distal tarsal; **etr**, external trochanter; **fe**, femur; **ft**, femoral
186 trochanter; **fi**, fibula; **fib**, fibulare; **fr**, frontal; **glf**, glenoid fossa; **hb**, hypobranchial; **hu**, humerus;
187 **i**, intermedium; **icf**, internal carotid foramen; **il**, ilium; **isc**, ischium; **lac**, lacrimal; **mx**, maxilla;
188 **na**, nasal; **obs**, orbitosphenoid; **op-ex**, opisthotic-exoccipital complex; **pa**, parietal; **pm**,
189 premaxilla; **po**, postminimus; **pra**, prearticular; **pre**, procoracoid; **prf**, prefrontal; **pro**, prootic;
190 **ps**, parasphenoid; **pt**, pterygoid; **pub**, pubis; **qu**, quadrate; **ra**, radius; **rad**, radiale; **rl**, radial loop;
191 **sca**, scapulocoracoid; **sm**, septomaxilla; **sq**, squamosal; **st**, stapes; **stf**, stapedial foramen; **ti**,
192 tibia; **tib**, tibiale; **ul**, ulna; **uln**, ulnare; **vo**, vomer; **y**, element y.

193

194 **Results**

195 **Systematics & Description**

196 Order Urodela Duméril, 1806

197 Suborder Cryptobranchoidea Dunn, 1922

198 Family Hynobiidae Cope, 1859

199 Genus *Batrachuperus* Boulenger, 1878

200

201 Species *Batrachuperus londongensis* Liu & Tian, 1978

202

203 **Holotype.** CIB 65I0013/14380, a male adult with a total length of 265 mm, a snout-vent length
204 of 129 mm. The holotype is a neotenic individual, as it is sexually mature but retains gill slits
205 and a larval type of hyobranchium.

206 **Type locality.** Longdong Stream (N29°34'42.85"/E103°17'5.61"), at an elevation of 1300 m
207 above sea level, Mt. Emei (Emeishan), Sichuan Province, China.

208 **Known distribution and habitat.** The species was previously thought to be known only from
209 Longdong Stream, a mountain stream associated with the Longdong Cave at 1200 m–1300 m
210 above sea level (Fei et al., 2006); however, a molecular systematics study has shown that
211 populations previously identified as *B. pinchonii* from the nearby Mt. Wawushan in Hongya
212 County and Mt. Nibashan in Hanyuan County may pertain to *B. londongensis* (Fu & Zeng,
213 2008). Based on field observations at the type locality, live individuals of the Longdong Stream
214 Salamander often hide under rock cover in the mountain stream, and they feed on fresh-water
215 shrimp, aquatic insects and insect larvae (Fei, Ye & Jiang, 2010).

216 **Diagnosis.** *Batrachuperus londongensis* can be distinguished from the type species
217 *Batrachuperus pinchonii* and all other congeneric species in having a unique combination of the
218 following osteological features: alary process of premaxilla barely contributing to border of
219 anterodorsal fenestra (shared with *B. tibetanus*); suture between nasal and frontal located at the
220 level of anterior border of orbit; frontal extending far posteriorly, terminating at the level of otic
221 process of pterygoid; vomers widely separated from one another, lacking a midline contact
222 (unique); vomerine teeth four to eight in number, arranged in a straight line that is strongly



223 oblique and nearly vertical in orientation (unique); ascending process of palatoquadrate ossified
 224 as a short pillar propping lateral edge of parietal behind orbit (shared with *B. karlschmidti* and *B.*
 225 *taibaiensis*); radial loops stemming from basibranchial I not crossing one another; presacral
 226 vertebrae 18 in number; scapular blade bearing prominent posterodorsal process for insertion of
 227 a levator muscle of the scapula (unique); ischial plate is penetrated by a small nerve foramen,
 228 and the ischial spine is clearly more elongated than in other species.

229 **Taxonomic remarks.** In the literature, the species epithet has been confusingly spelled as
 230 *Batrachuperus londongensis* (e.g., Liu & Tian, 1978; Liu et al., 1978; Fu et al., 2001; Wu & Xie,
 231 2004; Fei et al., 2006; Fei, Ye & Jiang, 2010, 2012) and *Batrachuperus longdongensis* (e.g., Liu
 232 & Tian, 1983 in Fei, Ye & Tian, 1983; Fei & Ye, 1984; Song et al., 2001). Judging from the
 233 published literature regarding the two available names differing in spelling, it is clear that the
 234 former is valid and the latter invalid owing to its status as a “nomen nudum” (Fei et al., 2006).

235 The validity of ~~the nomenclatural status of the~~ species name *Batrachuperus londongensis*
 236 was established by Liu & Tian (1978) in Liu et al. (1978). The year before this publication, the
 237 same authors (Liu & Tian, 1977) first published the species name spelled as “*Batrachuperus*
 238 *longdongensis*” in a taxonomic key brochure without a type designation, description, or
 239 illustration (see ICZN, 1999: art. 13); for that reason, the name “*Batrachuperus longdongensis*”
 240 Liu & Tian, 1977 is considered a nomen nudum (Fei et al., 2006). Unfortunately, Liu & Tian
 241 (1983, in Fei, Ye & Tian, 1983) “re-published” the invalid name “*Batrachuperus longdongensis*”
 242 and labeled it as a new species. Although the latter publication provided some detailed
 243 information on the species, “*Batrachuperus longdongensis*” Liu & Tian 1983 cannot be
 244 considered as the original spelling, but is a junior homonym of the nomen nudum
 245 “*Batrachuperus longdongensis*” Liu & Tian 1977. Fei et al. (2006) evidently chose to adopt

246 *Batrachuperus londongensis* as the original spelling in a valid publication by Liu & Tian (1978).
 247 Moreover, the species name *Batrachuperus londongensis* is in prevailing usage in the current
 248 literature (e.g., Fei et al., 2006; Fei & Ye, 2017; Fu & Zeng, 2008; Fei, Ye & Jiang, 2010, 2012;
 249 AmphibiaWeb, 2017; Frost, 2017; IUCN, 2016).



250

251 External morphology



252 Fluid-preserved specimens provide information on external morphology except for coloration.
 253 Male adults of *Batrachuperus londongensis* have been measured at 190 mm–265 mm in total
 254 length, and female adults at 183 mm–232 mm (Fei et al., 2006). Labial folds are well developed,
 255 partly covering the lower lips; gular folds are arched posteriorly to demarcate the head from the
 256 trunk. Neotenes have one to four pairs of gill slits, whereas in postmetamorphic individuals the
 257 gill slits are closed.

258 The presence or absence of eyelids and ring-shaped scleral cartilages in the eye are
 259 characters both ontogenetically and ecologically significant. Movable eyelids are normally
 260 developed at metamorphosis for adult life on land, but are often lacking in larvae and in those
 261 adults that are obligate neotenes (Duellman & Trueb, 1986). However, the ring-shaped scleral
 262 cartilage is partly resorbed at metamorphosis in *Hynobius* and *Onychodactylus* (Okajima &
 263 Tsuaki, 1921), while the extent of resorption of the scleral cartilage in other hynobiids is largely
 264 unknown (Rose, 2003). Our observations indicate that *Batrachuperus londongensis* has movable
 265 eyelids but lacks scleral cartilages in both neotenes and postmetamorphic individuals. Although
 266 developmental information is still unavailable, we infer that it is likely that scleral cartilages are
 267 fully resorbed at metamorphosis or at sexual maturity as a normal developmental pattern as in
 268 other hynobiids. Because the species is facultatively rather than obligately neotenic, possession

of movable eyelids may be indicative of their all-season aquatic life style being a secondary adaptation.

The trunk region is more or less cylindrical, having 12–14 costal grooves on each side along the trunk. A dorsal vertebral groove runs between the head and the base of the tail. The tail is one-half or slightly longer than one-half of total length. The tail has a cylindrical base, but becomes bilaterally compressed posteriorly, with evident dorsal and ventral fin folds extending distally. The end of the tail displays a rounded outline in lateral view (Fei & Ye, 2001). Toes in the hind limb are reduced to four (Fei et al., 2006; Fei & Ye, 2001), although occasional developmental anomalies are found in some individuals (see below). Terminal digits are claw-like, covered with a black cornified epidermal sheath.

Dermal skull roof

The skull roof is flat, longer than wide as in other congeneric species (Fei et al., 2006). The snout follows the contour of the maxillary arc: most specimens display a squarish outline, in contrast to the rounded snout in other congeneric species (e.g., *Batrachuperus pinchonii*, *B. karlschmidti*, *B. tibetanus*). The maximum width of the snout across the anterior borders of orbits is much narrower than the maximum width of the skull at the cranio-mandibular joints, thus giving a more or less trapezoidal outline of the skull roof in dorsal view. This outline differs from that in *B. pinchonii*, which has a more rounded snout than *B. londongensis*, and displays significant differences in the maximum width of the snout and at the back of the skull.

The paired premaxillae contact each other medially to close the anterior border of a large anterodorsal fenestra (de Beer, 1937: cavum internasale) in the skull roof and an anteromedial fenestra in the palate. The pars dentalis as the tooth-bearing part of the premaxilla forms the

anterior wall of the snout between the external nares, but its lateral extension articulates with the maxilla to form the medial half of the ventral border of the narial opening. The anterior surface of the premaxilla is penetrated by several small foramina. The pars dorsalis (alary process) of the premaxilla ascends from the midlength of the pars dentalis, with the entire spine of the process set in a groove on the anterodorsal surface of the nasal bone; therefore, the alary process essentially contributes no part to the lateral border of the anterodorsal fenestra. A similar pattern is seen in *B. tibetanus* (FMNH 5901), but not in other species of the genus.

The paired nasals are strongly widened to display a dimension almost twice the width of the frontals, a plesiomorphic feature in urodeles as commonly seen in other hynobiids (Dunn, 1923; Gao & Shubin, 2012; Jia & Gao, 2016a). In dorsal view, the nasal is a large plate, irregular in shape, meeting its counter element along a midline suture. The nasal has an anterior process, which is medially notched for the large anterodorsal fenestra and laterally notched for the narial opening. A lateral process of the nasal is in limited contact with the lacrimal, because a large part of the latter bone overlaps the prefrontal (Fig. 2). The dorsal surface of the nasal is smooth, but is penetrated by several tiny foramina (foramen mediale nasi of Francis, 1934) for passage of ultimate twigs of the mesial branch of the ophthalmicus profundus nerve (CN V) as seen in *Salamandra* (Francis, 1934). The nasal posteriorly overlaps the frontal extensively, and laterally meets with the lacrimal and prefrontal. In dorsal view, the suture between the nasal and frontal is located at the level of the anterior borders of the orbits.

The paired frontals are strongly elongated posteriorly, with a straight or slightly sigmoid sutural contact along the midline. The paired elements occupy much of the interorbital area of the skull roof, but form only a small part of the medial border of the orbit, with a large part of the border furnished by the parietal. The frontal articulates with the nasal anteriorly and with the

prefrontal anterolaterally. Immediately behind the posterior process of the prefrontal, the lateral border of the frontal curves downward to articulate with the orbitosphenoid; however, this contact is limited to only the anterior one-third of the orbitosphenoid, with the posterior two-thirds of the latter in contact with the parietal (Figs. 3,4). This short contact between the two elements is also seen in *B. karlschmidtii*, whereas in all other congeneric species the prefrontal contacts over one-half of the dorsal margin of the orbitosphenoid (Figs. 3,4). Posteriorly, the frontal overlaps the parietal extensively, with a strongly elongate posterior process extending to the level of the medial (otic) process of the pterygoid. This strong posterior extension of the frontal differs significantly from all other congeneric species, in which the frontal is proportionally shorter and terminates roughly at the midlevel of the orbit (e.g., FMNH 49380: *B. karlschmidtii*; FMNH 5901: *B. tibetanus*). Along the medial border of the orbit, the lateral margin of the frontal curves downward to meet the orbitosphenoid and the anterolateral process of the parietal.

The parietal is the largest element in the skull roof, but is extensively overlapped anteriorly by the posterior extension of the frontal. The paired parietals meet at a straight or slightly curved midline suture, and have parallel lateral borders forming most of the medial rim of the orbit. The main part of the parietal table, however, is expanded bilaterally to form robust lateral “boots” in articulation with the squamosals. The posterior part of the parietal table is rugose dorsally, and posteriorly bears a bony ridge that curves anteriorly to house a deep fossa (cervical epaxial fossa) for attachment of the intervertebral epaxial muscles (Carroll & Holmes 1980; Duellman & Trueb, 1986; Elwood & Cundall, 1994). Slightly anterior to the lateral boot of the parietal, the lateral surface of the parietal is pierced by a tiny foramen for the passage of the trochlear nerve (CN IV; Gaupp, 1911) as clearly seen in several specimens (e.g., CIB

65I0013/14380, 14381, 14504, 14507, 14509). This foramen has been identified in all other congeneric species that we have examined (*B. karlschmidtii*, *B. taibaiensis*, *B. tibetanus*, *B. pinchonii*, *B. yenyuanensis*) in this study and has also been reported in several other salamanders (e.g., Francis, 1934: *Salamandra*; Wake, 2001: *Dicamptodon*; AmphibiaTree, 2008: *Ambystoma*).

In both dorsal and lateral views, the parietal table sends an elongate anterolateral process pinched between the frontal and orbitosphenoid (Figs. 3,4). Anteriorly, the pointed end of this process terminates slightly anterior to the midlevel of the orbitosphenoid. At the posterior border of the orbit, the parietal develops a short triangular process, which is ventrally directed in contact with a distinct pillar-like bone that in turn is ventrally in contact with the pterygoid. This small pillar is identified as the perichondral ossification of the ascending process of the palatoquadrate, and the presence of such a distinct bony element in *Batrachuperus londongensis* differs from all other congeneric species but *B. karlschmidtii* and *B. taibaiensis* (see below).

The prefrontal is a robust element, set at an oblique position in front of the large orbit. The prefrontal meets the nasal and frontal medially; it underlies the lacrimal anteriorly and the facial process of the maxilla laterally. The posterolateral margin of the prefrontal is curved to form the anterodorsal rim of the orbit. The prefrontal has a well-developed posterior process that extends far posterior to the nasal-frontal suture. A similar pattern is seen in *Batrachuperus tibetanus*, but this process is much shorter in other congeneric species (*B. karlschmidtii*, *B. taibaiensis*, *B. pinchonii*, *B. yenyuanensis*). A prefrontal is normally present in most salamanders, but is absent in proteids, sirenids, and some but not all plethodontids (Trueb, 1993; Reilly & Altig, 1996; Rose, 2003).

360 The lacrimal is a narrow and slightly elongate plate, with its main part overlapping the
 361 prefrontal. The lacrimal is essentially rectangular, similar to that in *B. tibetanus* and *B.*
 362 *yenyanensis*, but differing from that in other congeneric species, in which the lacrimal is
 363 triangular with a pointed anterior end (*B. pinchonii* and *B. taibaiensis*) or more or less “L”-
 364 shaped with a short process bending posteromedially (*B. karlschmidtii*). In *B. londongensis*, the
 365 lacrimal has a limited contact medially with the nasal, but is in an extensive sutural articulation
 366 laterally with the facial process of the maxilla. The canal for the nasolacrimal duct (ductus
 367 nasolacrimalis) opens posteriorly on the dorsal surface of the lacrimal, with the anterior foramen
 368 opening on the anteroventral side of the lacrimal. As a common feature seen in most of
 369 *Batrachuperus* species, the lacrimal anteriorly enters the border of the external naris, but is
 370 posteriorly blocked by the prefrontal-maxillary contact from entering the border of the orbit (Fig.
 371 2). In other hynobiids, the lacrimal variably enters the naris only (e.g., *Salamandrella*), enters
 372 the orbit only (e.g., *Pachyhynobius*, *Paradactylodon*, some but not all species in *Hynobius*), or
 373 enters both the naris and orbit (e.g., *Liua*, *Onychodactylus*, *Pseudohynobius*, *Ranodon*, some
 374 species of *Hynobius*).

375 The maxilla is extremely short, but massively built, laterally covering the facial area of
 376 the skull. The pars dorsalis of the maxilla is a robust process that widens between the narial
 377 opening and the orbit. The process has an extensive sutural articulation with the lacrimal but a
 378 limited contact with the prefrontal posterior to the lacrimal. The lateral wall of the maxilla is
 379 slightly convex, and in some specimens (e.g., CIB 14485, 14509) is penetrated by a small
 380 foramen anteriorly close to the narial rim. Ventral to the narial opening, the anteroventral
 381 process of the maxilla articulates with the premaxilla to form one-half of the ventral border of the
 382 naris. The posterior border of the pars dorsalis forms a part of the orbital rim, with the remaining

part furnished by the prefrontal. On the inner side of the pars dorsalis, a deep groove leads to a small opening of the infraorbital canal, through which passes the superior alveolar branch of the trigeminal nerve (CN V) and its associated blood vessels as in other salamanders (Francis, 1934). In both neotenic and postmetamorphic individuals, the short posteroventral process of the maxilla terminates at a level far anterior to the midlevel of the orbit. The short maxillary tooth row contains no more than 18 teeth. The tooth row terminates close to the posterior extremity of the maxilla.

The septomaxilla is a small bone exposed anteromedial to the narial border of the maxilla. A septomaxilla is present in all hynobiids, and is also present in some other groups of urodeles (Rose, 2003: ambystomatids, dicamptodontids, rhyacotritonids, and some but not all plethodontids). The absence of this element in several groups (sirenids, cryptobranchids, amphiumids, and proteids) cannot be simply explained as a “paedomorphic loss” (contra Duellman & Trueb, 1986), as it is present in the Jurassic neotenic salamanders *Beiyanerpeton* and *Qinglongtriton* (Gao & Shubin, 2012; Jia & Gao, 2016b). In this study, all known specimens of *Batrachuperus londongensis* consistently display the septomaxilla in both neotenic and postmetamorphic adults. Ontogenetically, the septomaxilla is ossified immediately before or during metamorphosis in *Onychodactylus* (Vassilieva, Poyarkov & Iizuka, 2013), *Ranodon* (Schmalhausen, 1968; Lebedkina, 2004), *Salamandrella* (Schmalhausen, 1958; Lebedkina, 1964; Regel, 1970), and *Hynobius* (Vassilieva et al., 2015).

Suspensorium

The squamosal is roughly T-shaped, with its widened proximal end in articulation with the lateral “boot” of the parietal, and a transverse bar extending ventrolaterally over the quadrate. In

406 dorsal view, the transverse bar is set at right angles in relation to the sagittal plane of the skull; in
 407 **occipital view**, however, the transverse bar is set in an oblique position, sloping ventrolaterally at
 408 a 45 degree angle towards the cranio-mandibular joint. At the proximal end, a blunt otic process
 409 projects anteriorly to articulate with the prootic, and a triangular process projects posteriorly with
 410 its tip in contact with the opisthotic-occipital complex (Fig. 2). The squamosal is slightly convex
 411 dorsally, but concave ventrally to embrace a large part of the quadrate.

412 The quadrate as a principal element of the suspensorium extends transversely beneath the
 413 squamosal. In contrast to the squamosal, the quadrate has a widened lateral end and a medial
 414 process extending towards the stapes (columella). In dorsal view, the lateral end of the quadrate
 415 is exposed beyond the distal end of the squamosal, where the quadrate thickens ventrally to form
 416 a cartilage-lined saddle for articulation with the articular in the mandible. From the distal end, a
 417 short and flat process overlaps the posterolateral process of the pterygoid. As revealed in CT
 418 images of several specimens (e.g., CIB 65I0013/14380, 14381, 14507), a tiny quadrate foramen
 419 pierces the base of the pterygoid process for passage of a branch of the posterior condylar artery
 420 and vein as generally seen in other tetrapods (Olson, 1966). A quadrate foramen has been
 421 identified in the Early Cretaceous hynobiid-like salamander *Nuominerpeton* (Jia & Gao, 2016a),
 422 whereas the occurrence of the foramen in extant hynobiids needs to be investigated thoroughly to
 423 understand its phylogenetic significance. The ascending process of the quadrate extends beneath
 424 the squamosal, **approaching but not reaching the otic region (stapes)**. Ossification of the
 425 quadrate occurs in all salamanders except sirenids (Rose, 2003). Ontogenetic ossification of the
 426 quadrate in different hynobiid species can be variably before (Suzuki, 1932; Lebedkina, 2004;
 427 Jia & Gao, 2016a), during (Lebedkina, 1964) or immediately after metamorphosis (Vassilieva et
 428 al., 2015).



429 The pterygoid is roughly boomerang-shaped in ventral view (Fig. 4). The anterolateral
 430 (palatal) process is elongated, extending to a point slightly anterior to the midlevel of the orbit;
 431 thus, the ligamentous connection with the maxilla is extremely short. As a common pattern in
 432 other salamanders, all hynobiids have a ligamentous connection between the maxilla and
 433 pterygoid, with the exception of *Pachyhynobius*, in which a bony contact between the two
 434 elements is established (Fei et al., 2006). In *B. londongensis*, the ventral surface of the
 435 anterolateral process is smooth, but the dorsal surface is grooved for a slender rod of cartilage
 436 (processus pterygoideus of the palatoquadrate), which extends along the entire length of the
 437 anterolateral process of the pterygoid.

438 The posterolateral (quadrate) process of the pterygoid is slightly shorter than the
 439 anterolateral process. A large part of the former process underlays the quadrate to reinforce the
 440 cranio-mandibular joint. In addition to serving as a part of the suspensorium, the pterygoid also
 441 provides attachment for adductor muscles, including the pterygoideus head of the adductor
 442 mandibulae internus (Carroll & Holmes, 1980). The medial (otic) process of the pterygoid is
 443 short, but turns dorsally to meet a small pillar (ossified ascending process of the palatoquadrate);
 444 thus, the process has no bony contact with the parasphenoid. Lack of a synostotic contact
 445 between the pterygoid and parasphenoid is a common pattern in all other *Batrachuperus* species
 446 except *B. yenyuanensis*, in which the pterygoid directly meets the parasphenoid below the
 447 prootic (FMNH 49371).

448 As mentioned above, it is of special interest to note the presence of a short pillar propping
 449 the parietal immediately anterior to the prootic (Figs. 2,3). In our knowledge, this short pillar
 450 represents the perichondral ossification of the ascending process of the palatoquadrate (Trueb,
 451 1993: metapterygoid; Rose, 2003: epipterygoid). The short pillar is set in a vertical or slightly

oblique orientation, dorsally in articulation with a downward process of the parietal and ventrally with the upward medial process of the pterygoid. In other salamanders, the ascending process of the palatoquadrate normally remains unossified, whereas a “certain amount of perichondral ossification” of the process has been documented in *Salamandra* (Francis, 1943: 26) as part of the suspensorium.

In this study, all of the adult specimens of *Batrachuperus londongensis* that we have examined consistently show the presence of this pillar in the same position, and the same contact patterns of the bone with the parietal and pterygoid can be seen in both dorsal and lateral views (Figs. 2,3). CIB 14500 is a postmetamorphic juvenile, which shows that this pillar is not yet ossified, as the individual also lacks ossification of the articular in the lower jaw (see below). On the other hand, *B. karlschmidti* (FMNH 49380) and *B. taibaiensis* (CIB 20040235) are the two congeneric species that show the presence of this bone and the same articulation patterns as in *B. londongensis*. In other hynobiids, ossification of the pillar as part of the suspensorium is also seen in *Paradactylodon mustersi* (FMNH 49380) and *Pseudohynobius flavomaculatus* (CIB 79I0107/17344). Whether this ossification represents a plesiomorphic feature with a homologous origin or is it a derived state independently acquired needs to be investigated in a phylogenetic analysis.

Palate and braincase


Formation of the palate involves the partes palatina of the premaxillae and maxillae, the vomers, and the anterior portion of the parasphenoid. The partes palatina of the premaxillae are the lingual shelves of the premaxillae that meet at the midline to close the anterior border of the large palatal fenestra. The fenestra (Schmalhausen, 1968: intervomerine cleft; Trueb, 1993:

475 anteromedial fenestra) is the palatal opening for the intermaxillary gland (Schmalhausen, 1968).
 476 Laterally, the pars palatina of the maxilla contacts the vomer to complete the lateral rim of the
 477 palate.

478 In several neotenic individuals (e.g., CIB 14381, 14382, 14509), the ossified palatine is
 479 retained as a discrete element either in articulation with or free from the anterior process of the
 480 pterygoid on both sides of the palate (Fig. 4). In these specimens, the palatine occurs as a small
 481 plate or a slender bar; ~~toothless in palatal view.~~ The palatine is entirely resorbed in all other
 482 hynobiids in the adult stage as is commonly seen in other salamanders except sirenids
 483 (Worthington & Wake, 1971; Smirnov & Vassilieva, 2002a; Rose, 2003); therefore, the retention
 484 of this element as an ossification in some but not all specimens in *Batrachuperus londongensis*
 485 can be interpreted as an ontogenetic feature. This interpretation is supported by the hynobiid-
 486 like fossil salamander *Nuominerpeton aquilonaris* of Early Cretaceous age from China, which
 487 displays normal resorption of the palatine at metamorphosis (Jia & Gao, 2016a). Furthermore,
 488 none of the specimens of *B. londongensis* that we examined have shown a separate palatine at a
 489 postmetamorphic stage, and large neotenic individuals (e.g., CIB 65I0013/14380, 14484, 14485)
 490 also lack this element. Because those specimens having a discrete palatine are apparently adult
 491 individuals, ontogenetic resorption of the element in these individuals seems to be delayed until
 492 after sexual maturity.

493 The vomer is a large plate, irregular in shape, slightly longer than wide. The two vomers
 494 are widely separated from one another, thus allowing the parasphenoid to enter the posterior
 495 border of the anteromedial fenestra. This pattern is consistently observed in all specimens, and
 496 thus is recognized in this study as a unique feature different from all other species in
 497 *Batrachuperus* and other hynobiids as well. Jömann, Clemen & Greven (2005: fig. 33) figured

Ranodon sibiricus at the adult stage as showing no midline contact of the vomers, but this was probably based on juvenile or subadult specimens (Jömann, Clemen & Greven, 2005: table 1: TL= <150 mm) as the nasals are widely separated (Jömann, Clemen & Greven, 2005: fig. 32) in contrast to the condition in fully grown adults (maximum TL= 250 mm) as figured in Fei et al. (2006: fig. 67). In *B. londongensis*, the medial border of the vomer is slightly concave, forming the entire lateral margin of the anteromedial fenestra (Fig. 4). Posterolaterally, the vomerine plate is notched for the choana, with a small triangular process projecting towards the orbit to embrace the notched choana. However, a retrochoanal (postchoanal) process is absent, as a laterally directed process to block the posterior border of the choana is clearly lacking. Another projection, medially attached to the parasphenoid, represents the posterior process of the vomer (Fig. 4).

A large part of the ventral surface of the vomer is smooth, except for a small tooth-bearing area medial to the choana. The vomerine teeth are four to eight in number, arranged in a linear fashion to form a straight row. The two vomerine tooth rows are widely separate but slightly oblique, convergent anteriorly and divergent posteriorly. This arrangement differs from most other congeneric species: in them the vomerine tooth row is more or less arched and parallel to the maxillary tooth row. Close to the maxilla-vomer suture, the vomer is penetrated by two to **three small foramina** observed in several specimens (CIB 65I0013/14380, 14381, 14504, 14509), probably for passage of the ramus ventralis of the trigeminal nerve (CN V) and the ramus palatinus of the facial nerve (CN VII) to supply the mucous membranes of the mouth, as in other salamanders (Francis, 1934: *Salamandra salamandra*; Cloete, 1961: *Rhyacotriton olympicus*).

The parasphenoid as a dermal bone forms a large median plate, roughly rectangular in outline, with straight lateral borders parallel to one another. The anterior process of the parasphenoid contributes to part of the palate and closes the posterior border of the anteromedial fenestra (Fig. 4). The anterolateral part of the parasphenoid bears a flat facet for attachment of part of the vomer posterolateral to the anteromedial fenestra. The lateral edge of the parasphenoid curves dorsally, with a narrow groove in articulation with the ventral edge of the orbitosphenoid. Posteriorly, the basal plate of the parasphenoid is widened to form the lateral ala that floors the otic capsule. Close to the anterolateral border of the basal plate, a pair of internal carotid foramina penetrates the parasphenoid for passage of the internal carotid arteries. As observed in several specimens (CIB 65I0013/14380, 14381, 14504, 14507, 14509, 14482), more than one foramen may occur on either side of the parasphenoid, possibly indicating minor branches of the artery. The lateral ala has no bony contact with the otic process of the pterygoid, but is in articulation with the prootic (Fig. 4). The posterior end of the parasphenoid forms a blunt posteromedian process, which furnishes the ventral rim of the foramen magnum.

The orbitosphenoid (sphenethmoid) as an endochondral bone is a rectangular plate that covers a large part of the anterolateral wall of the braincase. The bony plate dorsally articulates with the frontal and parietal, but in some specimens (e.g., CIB 65I0013/14380) it also articulates with the prefrontal (Figs. 3,4). The entire ventral edge of the orbitosphenoid meets the parasphenoid. The anterior edge of the orbitosphenoid is vertical, forming a straight border of the orbitonasal fenestra; the posterior border, however, is deeply notched for the optic foramen, carrying the optic nerve and its associated vessels (Francis, 1934; Fox, 1959). There is no foramen in the orbitosphenoid for passage of the oculomotor nerve (CN III); instead, this nerve passes through the optic-oculomotor commissure, which is covered by cartilaginous tissues

posterior to the orbitosphenoid. This pattern of cranial nerves exiting through the anterolateral wall of the braincase has been recognized as a diagnostic feature of the Hynobiidae (Jia & Gao, 2016a), differing from the sister group Cryptobranchidae, in which the optic foramen is fully surrounded by the bony rim of the orbitosphenoid.

No operculum, bony or cartilaginous, is identified in any of the specimens. The stapes (columella) has a massive and disc-like footplate covering the foramen ovalis. The stylus is extremely short, fused with the footplate proximally but with a small facet at its obtuse distal end for attachment of the ligamentum squamoso-cumellare, which connects the stapes with the quadrate and squamosal (Kingsbury & Reed, 1909). A stapelial foramen is unexpectedly present on both sides in two specimens (CIB 65I0013/14380, 14381; both neotenic individuals), penetrating the stylus horizontally. In two other specimens (CIB 14507, 14509; both postmetamorphic individuals), a foramen penetrates left and right stapes, as well. However, none of the other specimens, neotenic or postmetamorphic, show the presence of the foramen. Therefore, the stapelial artery and/or the hyomandibular trunk of the facial nerve (CN VII) in this species can variably pass through the stapelial foramen or below the short stylus. A similar condition is known for *Ranodon sibiricus*: Schmalhausen (1968) described both present and absent conditions of the stapelial foramen from specimens that he observed. Although Trueb & Cloutier (1991) interpreted the absence of a stapelial foramen as a batrachian synapomorphy, its presence in some salamanders is more likely to be a plesiomorphic feature for Urodela because it also occurs in the stem caudate *Karaurus* (Ivachnenko, 1978; Estes, 1981). Furthermore, the foramen is found in the Late Jurassic salamandroids *Beiyanerpeton* and *Qinglongtriton* from China (Jia & Gao, 2016b). The discovery of the presence of this foramen in some but not all

postmetamorphic individuals in *Batrachuperus londongensis* casts more doubt on our understanding of the evolution of this character.

A separate operculum is absent in *B. londongensis*, as is common in other hynobiids (Monath, 1965; Rose, 2003). An operculum is figured as present in *Liua shihi* (Zhang, 1985) and *Ranodon sibiricus* (Jömann, Clemen, & Greven, 2005: fig. 34); however, the element that is labeled in both cases seems to be the stapes as it has a rounded foot-plate fused with the stylus.

The prootic is irregular in shape, covering the lateral wall of the anterior portion of the otic capsule. The element dorsally articulates with the parietal, but a small part of its dorsal rim underlays the squamosal as well. Ventrally, the prootic articulates with the lateral ala of the parasphenoid. In lateral view, the alary process (optic process) of the prootic is a small flap directed anterodorsally; the inferior process (basal process) of the prootic is more or less triangular, with its ventral edge in articulation with the parasphenoid (Fig. 3). A large foramen faciale penetrates the lateral surface of the prootic for passage of the facial nerve (CN VII).

The opisthotic and exoccipital are fully fused to form an opisthotic-exoccipital complex covering the posterior wall of the braincase. The complex dorsally articulates with the parietal and ventrally with the parasphenoid; in dorsal view, it is swollen posterolaterally as the housing of the auditory capsule. The opisthotic portion of the complex borders the fenestra ovalis anteriorly, whereas its exoccipital part borders the foramen magnum posteromedially and bears the occipital condyle posteriorly for articulation with the cotyle of the atlas. At the base of the occipital condyle, the complex is penetrated by the foramen post-oticum (Francis, 1934) for the combined glossopharyngeus-vagus nerves (CN IX + X). In all hynobiids the opisthotic-exoccipital complex is fused and the prootic free (Carroll & Holmes, 1980; contra Trueb, 1993: three separate elements), except for *Onychodactylus*, in which the prootic is fused to the

opisthotic-exoccipital complex (Smirnov & Vassilieva, 2002b; Vassilieva et al., 2013). In occipital view, the foramen magnum is roughly triangular in outline. The dorsal rim of the foramen has a median gap for the cartilaginous tectum synoticum below the parietals. The ventral border of the foramen magnum is largely supplied by the posteromedian process of the parasphenoid.

Mandible

As in all cryptobranchoids (hynobiids and cryptobranchids), the lower jaw of *Batrachuperus londongensis* consists of the dentary, prearticular, angular and articular. In addition, a small posterior mental process seen in all specimens at the symphysis gives a clear indication of the co-ossification of a mentomeckelian element with the dentary (Fig. 5).

The dentary is the largest bone in the mandible, covering most of its lateral and ventral aspect. The lateral surface of the dentary is smooth, slightly swollen along the lower border but weakly concave along the tooth row. A large foramen is often located at a position slightly posterior to the midlevel of the dentary tooth row (Fig. 5). This foramen marks the passageway for the mandibularis externus nerve (CN V₃), supplying both the skin and the muscle (M. intermandibularis) between the two rami of the lower jaw (Francis, 1934). Posteriorly, the dentary terminates at a robust process below the cranio-mandibular joint.

Posteroventral to the dentary, the angular bone is exposed in medial, ventral and lateral views. As observed in both lateral and ventral views, the angular is slightly thickened posteriorly but narrows anteriorly, where it is wedged between the prearticular and the dentary. The pointed anterior process terminates at a level slightly posterior to the anterior extremity of the anterolateral process of the pterygoid, and the thickened posterior end forms the

posteroventral extremity of the mandible. In medial view, a small angular foramen opens anteroventrally at the angular-prearticular suture, close to the anterior end of the angular and below the coronoid process of the prearticular.

The prearticular is a large element covering most of the medial aspect of the jaw. Anteriorly, the bone terminates at a point close to the mandibular symphysis. Posterodorsally, the prearticular rises to form a large ascending process (coronoid process) for insertion of the adductor mandibulae internus muscle. The process slopes downward posteriorly and continues as a ridge that attaches to the medial side of the articular at the glenoid fossa. Below and posteroventral to the coronoid process, the prearticular is penetrated by one or two foramina (inferior dental foramina) for passage of the inferior alveolar ramus of the facial nerve (CN VII) and the alveolar artery (Francis, 1934). There is often a third foramen for the same nerve and vessel opening more anteroventrally at the tip of the angular bone.

The articular is well ossified in adults as in other extant species and fossil relatives of hynobiids but is absent in cryptobranchids (Reese, 1906; Rose, 2003; Jia & Gao, 2016a). In comparison to the angular, the articular is slightly shorter but more stoutly built. In dorsal view, it sends an anterior process between the prearticular and dentary, terminating at an obtuse tip medial to the coronoid process of the prearticular (Fig. 5). The slightly expanded posterior part of the articular is in articulation with the quadrate. As revealed from CT-scanned images, a tube-like canal runs horizontally through the articular for the passage of the ramus hyomandibularis of the facial nerve (CN VII); whether this pattern occurs in other congeneric species and other hynobiids needs to be thoroughly investigated. Ontogenetically, the articular ossifies slightly later than the septomaxilla after metamorphosis (Smirnov & Vassilieva, 2002; Rose, 2003; Lebedkina, 2004; Vassilieva, Poyarkov & Iizuka, 2013; Vassilieva et al., 2015); thus, presence

of a bony articular is a clear indication of maturity in fossil and extant hynobiids (Jia & Gao, 2016a). In this study, CIB 14500 is a postmetamorphic juvenile (TL= 110 mm; SPL= 60.24 mm), which displays a typical postmetamorphic pattern of the hyobranchium but shows no ossification of the articular. Once again, comparison of this with other specimens indicates that the articular is ossified after metamorphosis in *Batrachuperus londongensis*. This ossification sequence of the articular is similar with some other hynobiids, for example, *Onychodactylus japonicus* (Smirnov & Vassilieva, 2002) and *Hynobius formosanus* (Vassilieva et al., 2015), but differs from that in *Ambystoma*, in which the element is ossified at metamorphosis (Reilly, 1987).

Dentition

Tooth-bearing elements in *Batrachuperus londongensis* include the premaxilla, maxilla and vomer in the skull, and dentary in the mandible. The premaxilla carries seven to nine teeth; the tooth rows on both sides are slightly curved to form a broad arc, corresponding to the blunt snout. The maxilla carries 16–18 teeth, with the tooth row terminating at the posterior extremity of the maxilla.

As described above, each vomer bears a single tooth row containing four to eight teeth. The tooth row is essentially straight, but arranged obliquely medial to the choana with the two tooth rows slightly converging anteriorly. The tooth rows are set far apart from one another, corresponding to the separation of the vomers. Other palatal elements, including the parasphenoid and pterygoid, are entirely edentate.

The dentary tooth row is slightly longer than that of the maxilla, terminating posteriorly at a point slightly anterior to the coronoid process of the prearticular. The dentary teeth are 20–25 in number. All marginal teeth and vomerine teeth are pedicellate, with the basal pedicel and

crown separated by a poorly mineralized dividing zone. Tooth crowns are bicuspid as commonly seen in most salamanders.

Hyobranchial apparatus

The hyobranchial apparatus in *Batrachuperus londongensis* has been shown to have two different patterns related to life-history differences (Fei et al., 2006: fig. 69). The neotenic pattern retains some of the larval branchial arches, and thus displays more complex structures than in the postmetamorphic pattern (Fig. 6).

Cartilaginous elements cannot be observed in CT-scanned images, but can be detected in cleared and stained specimens (Fig. 6). A cornua is present as a partly mineralized median plate in the postmetamorphic pattern, whereas it is absent in neotenes (Fig. 6A,B). In both neotenic and postmetamorphic individuals, the paired radial loops stemming from basibranchial I (anterior copula) extend anteriorly, then curve laterally in continuation with the ceratohyal. Therefore, the paired radial loops do not cross one another, in contrast to *Batrachuperus pinchonii* and some other hynobiids (*Onychodactylus*, *Hynobius*, *Pseudohynobius*, *Pachyhynobius*), in which a figure 8-shaped pattern is formed by a complex crossing of the radial loops (Larson et al., 1996; Rose, 2003; Xiong et al., 2013b).

Basibranchial I (anterior copula) remains cartilaginous in both neotenic and postmetamorphic individuals as in all other hynobiids except *Onychodactylus*, in which the element is partly ossified as a short stub (Fukuda, 1930; Smirnov & Vassilieva, 2002; Xiong et al., 2013b). Presence or absence of basibranchial II (posterior copula, os thyroideum of Rose, 2003) was previously unknown for *Batrachuperus londongensis*. Observation of multiple specimens in this study reveals that basibranchial II is well ossified, displaying two different

680 patterns that may reflect developmental differences (see discussion below): most specimens have
 681 an anteriorly directed rod jointed with a transverse bar to form a simple inverted “T”-shaped
 682 structure; other specimens have a long anterior rod connected with a complex base, which
 683 displays multiple short branches directed posteriorly (termed here the “fork”-shaped pattern).
 684 None of the specimens on which this study is based shows an anchor-shaped basibranchial II, a
 685 configuration that has been recognized as a plesiomorphic condition for urodeles (Jia & Gao,
 686 2016b). The anchor-shaped basibranchial II occurs in the stem caudate *Karaurus* (Ivachnenko,
 687 1978; Estes, 1981), basal cryptobranchoid *Chunerpeton* (Gao & Shubin, 2003), and basal
 688 salamandroid *Beiyanerpeton* (Gao & Shubin, 2012). The plesiomorphic pattern is not seen in
 689 any extant hynobiids (see Xiong et al., 2013b), but occurs in the basal hynobiid *Nuominerpeton*
 690 (Jia & Gao, 2016a).

691 Hypobranchial I and ceratobranchial I remain separate in *Batrachuperus londongensis*, in
 692 contrast to the fusion in *B. pinchonii*, *B. tibetanus* (Fei et al., 2006) and several other hynobiids
 693 (*Ranodon*, *Hynobius*, *Pseudohynobius*, *Salamandrella*, *Liua*) (Fei et al., 2006; Zhang et al., 2009;
 694 Xiong et al., 2013b). Hypobranchial I in most specimens remain cartilaginous, but ossification
 695 of the element occurs in large neotenes (CIB 65I0013/14380, 14381). CIB 14504 is the only
 696 postmetamorphic individual that has it as a bony rod (Fig. 6B). Ceratobranchial I is increasingly
 697 ossified ontogenetically in neotenes (CIB 65I0013/14380, 14381, 14482, 14484, 14485, 14499),
 698 but it remains cartilaginous in all postmetamorphic individuals. ~~No matter~~ **bony** or cartilaginous,
 699 the distal end of ceratobranchial I is slightly hooked, bearing a small process that curves
 700 posterodorsally (Figs. 6,7).

701 Hypobranchial II and ceratobranchial II are both ossified as separate elements as in all
 702 other hynobiids (Fei et al., 2006; Xiong et al., 2013b). The former element is basically rod-like,

slightly thicker posteriorly than anteriorly; the shaft can be relatively straight or slight curved laterally. Ceratobranchial II is much longer than hypobranchial II, and often displays an expanded distal end, which is bilaterally compressed into a distal plate. This is especially the case in large neotenes, including the holotype. At midlength in the long rod, a prominent process projects dorsomedially for attachment of subarcualis rectus II as in *Amphiuma* (Erdman & Cundall, 1984). Ceratobranchial III and IV are entirely absent in postmetamorphic individuals (but see below), whereas they are present as bony elements in neotenes (Figs. 6,7). CIB 14487 is a postmetamorphic young adult (TL= 164 mm; SPL= 89.27 mm); its adulthood is indicated by ossification of the articular in the lower jaw, but it displays remnant ceratobranchial III in the process of being resorbed.

The ceratohyal in both postmetamorphic and neotenic individuals is distally ossified, with large adults showing more extensive ossification than smaller ones. In the holotype (CIB 65I0013/14380), the largest specimen known for the species (TL= 265 mm) and a neotene, over 60% of the ceratohyal is ossified as a robust element, leaving only the anterior one-third cartilaginous (Fig. 7). The ossified part of element has a prominent ridge posterodorsally for a ligamentous connection with the suspensorium (Trueb, 1993; Rose, 2003). Partial ossification of the ceratohyal is also seen in all other species of *Batrachuperus*: *B. pinchonii* (Zhang et al., 2009: fig. 24); *B. tibetanus* (FMNH 5901); *B. yenyuanensis* (FMNH 49371); *B. karlschmidtii* (FMNH 49380); *B. taibaiensis* (CIB 20040235). Among other hynobiids, partial ossification of the ceratohyal distally occurs in *Pachyhynobius shangchengensis*, *Liua shihi*, and *Ranodon sibiricus* (Zhang, 1985; Fei et al., 2006).

Axial skeleton



726 As consistently observed from all specimens **understudy**, the vertebral column consists of 18
 727 presacral vertebrae, including the atlas, plus a single sacral, three to four caudosacrals, and 29–30
 728 caudal vertebrae (Fig. 7). The number of the presacral vertebrae is different from the type
 729 species, *Batrachuperus pinchonii*, as well as all other congeneric species, which have 17
 730 presacrals (Zhang et al., 2009; Xiong et al., 2013a; but see Litvinchuk & Borkin, 2003: 16–17).
 731 Among other hynobiid species, the number of presacral vertebrae ranges from 15 in *Ranodon*
 732 *sibiricus* to 22 in *Onychodactylus fischeri* (Litvinchuk & Borkin, 2003).

733 In both dorsal and ventral views, the atlas is widened anteriorly to bear a pair of cotyles
 734 that receive the occipital condyles. Anteroventral to the cotyles is the odontoid process
 735 (tuberculum interglenoideum), which bilaterally articulates with the exoccipitals in the rim of the
 736 foramen magnum. Posterior to the odontoid process, the ventral surface of the atlas is penetrated
 737 by a pair of foramina for passage of the first pair of spinal nerves. The atlas bears no transverse
 738 process or free ribs.

739 In all trunk vertebrae, the centrum is more or less cylindrical and is deeply amphicoelous.
 740 There is no significant change in length of the centrum along the trunk series, and all trunk
 741 vertebrae bilaterally bear transverse processes that are directed posterolaterally. A shallow
 742 groove is visible on the posterior surface of the transverse process, indicative of fusion of the
 743 dorsal diapophysis with the ventral parapophysis. Because of this fusion, the articulation facets
 744 of the diapophysis and parapophysis are confluent for articulation with the uncapitate ribs.

745 All presacral vertebrae except the atlas bear free ribs. The ribs associated with the first
 746 three trunk vertebrae are more robust than the remaining ribs, having the distal end expanded for
 747 attachment of pectoral muscles. In addition, the first pair of ribs often bears a short uncinate
 748 process distally, so that the ribs are distally bifurcated (e.g., CIB 14482, 14484, 14485, 14487).

The ribs are similar in length for most of the trunk series, but the posterior four to five pairs are abruptly shortened, with the last pair being a remnant stub that is even shorter than the transverse process of the associated vertebra. All trunk ribs are essentially single headed, although a shallow groove can be recognized posteriorly on the rib head as indication of fusion of the dorsal tuberculum with the ventral capitulum. Possession of unicapitate ribs is a diagnostic feature of the suborder Cryptobranchoidea (Dunn, 1923; Duellman & Trueb, 1986; Gao & Shubin, 2012; Jia & Gao, 2016a).

The single sacral vertebra is roughly the same size as the presacrals, but the transverse process of the sacral is obviously more robust than that of the trunk vertebrae. The sacral rib is elongate to at least twice the length of the transverse process, and curves ventrally for a ligamentous connection with the ilium.

The three rib-bearing vertebrae following the sacral are identified as caudosacrals, with the first haemal arch bearer marking the position of the anus. CIB 14485 is the only examined specimen that displays four caudosacrals. These caudosacrals are roughly the same size as the sacral vertebra, but ribs associated with them are greatly reduced, being slightly shorter than the corresponding transverse process. Possession of three or more caudosacrals seems to be plesiomorphic in urodeles (Gao & Shubin, 2001, 2012; Jia & Gao, 2016b). The true caudal vertebrae following the caudosacral series are 28–30 in number in fully-grown adults. The caudal vertebrae normally have no free ribs, but occasionally remnant ribs occur in the first caudal in some specimens (CIB 14484, 14487). All caudal vertebrae but the posteriormost two or three ventrally bear a haemal arch, through which pass the haemal vessels.

Appendicular skeleton

772 ***Pectoral girdle and forelimbs***

773 A large part of the pectoral girdle remains cartilaginous, with only the scapulocoracoid co-
 774 ossified as a single unit. A co-ossified scapulocoracoid occurs in all other salamanders but
 775 sirenids, in which the scapula and coracoid remain separate (Noble, 1931). The scapulocoracoid
 776 in *Batrachuperus londongensis* has an extremely short scapular blade as in other species of the
 777 genus, but the dorsal border of the blade bears a distinct process projecting posterodorsally (Fig.
 778 8), a feature not seen in other *Batrachuperus* species. Because this process is consistently
 779 prominent in all specimens under study (e.g., CIB 14830, 14482, 14484, 14485, 14487), it is
 780 recognized here as a diagnostic feature of the species. Judging from its posterodorsal position, it
 781 unlikely served for the attachment of the opercular muscle, but more likely provided ligamentous
 782 attachment of a levator muscle of the scapular; whereas it is for the levator scapulae inferior or
 783 the intertransversarius capitis inferior needs to be further investigated (see Gaupp, 1898;
 784 Kingsbury & Reed, 1909; Goodrich, 1930; Monath, 1965). Anterior to this process, the dorsal
 785 border of the scapular blade displays an elliptical depression that received the suprascapular
 786 cartilage.

787 In the ventral part of the pectoral girdle, the procoracoid and coracoid are fully co-
 788 ossified to form a large plate, which is expanded anteroposteriorly and curved ventromedially.
 789 In lateral view, the anterior border of the coracoid plate is straight, but the ventral border is
 790 rounded. Both the anterior and ventral borders are grooved for attachment of the cartilaginous
 791 part of the procoracoid and coracoid, respectively. Close to the posterodorsal border of the
 792 coracoid plate is a large facet (glenoid fossa) formed by both the scapula and coracoid for
 793 articulation with the humerus. The glenoid fossa is roughly circular, but its anteroventral rim is
 794 deeply notched to receive the crista ventralis of the humerus (see below). Anteroventral to the

glenoid fossa, a small supracoracoid foramen (occasionally two openings) penetrates the coracoid plate for passage of the supracoracoideus nerve (from the second and third spinal nerves) and its associated vessels (Francis, 1934). In addition, it is interesting to note that some specimens (e.g., CIB 65I0013/14380, 14504) display partial ossification of what otherwise is the cartilaginous part of the procoracoid and coracoid (Fig. 8). Because extra ossification of these cartilaginous parts occurs only in very large specimens of both postmetamorphic and neotenic individuals, it can be viewed as a developmental feature but one that cannot be tied with neoteny or metamorphosis.

The humerus is significantly longer than the ulna or radius. Proximally on its extensor aspect, the crista dorsalis (dorsal crest) bears a prominent triangular or even knob-like projection, for insertion of the M. subscapularis (Francis, 1934). Proximally on the flexor aspect, the crista ventralis (ventral crest) is a large triangular process, projecting anteroventrally for attachment of the M. pectoralis and M. supra-coracoideus (Francis, 1934) and merging with the head of the humerus (or a facet in some specimens; see below). When the forelimb swings forward, the crista ventralis fits into the notch of the anteroventral rim of the glenoid fossa as mentioned above. Immediately ventral to the humeral head, a small but deep ventral depression marks the insertion of the flexor muscle M. humero-artibrachialis (Francis, 1934). In young adult specimens (e.g., CIB 14484, 14485, 14487), the humerus head is a cartilaginous cap, and thus, CT-scanned images show a shallow facet; in fully grown adults (e.g., CIB 65I0013/14380, 14381, 14482, 14504, 14509), the humeral head is ossified into a large spherical condyle. Among the latter, no postmetamorphic specimens show a cartilaginous cap, whereas only relatively small neotenic individuals show a cartilaginous condyle. Distally, the olecranon fossa on the extensor side of the humerus is extremely shallow, barely recognizable, but the fossa cubitalis ventralis on

the flexor side is a deep triangular depression, which receives the radius when the forearm is flexed. In relatively small neotenes, the radial and ulnar condyles are unossified, with the distal end of the humerus bearing two facets for attachment of the cartilaginous ulnar and radial condyles.

In the forearm, both the ulna and radius are straight, subequal in length and approximately two-thirds the length of the humerus. The proximal end of the ulna is more expanded than its distal end, and conversely the radius is a more expanded distally. Posterolaterally, the ulna bears a bony crest for attachment of the extensor of the forearm (*M. extensor antibrachii ulnaris*). The radius is distally in articulation with the radiale and intermedium. Close to its proximal end, the radius posterodorsally bears a prominent process for ligamentous attachment of the *M. humero-antibrachialis*, the main flexor muscle of the elbow (Francis, 1934). As described above for the humerus, in those specimens having a well-ossified humeral condyle, the epiphysis of the radius and ulna is also ossified, leaving no space for a cartilaginous cap.

Maximum ossification of the mesopodium in the forelimb displays a total of seven elements as observed in several specimens including the holotype (CIB 65I0013/14380, 14381, 14482, 14505, 14507, 14509), whereas other specimens (CIB 14484, 14485, 14487) have six ossified elements, with preaxial elements (radiale + element y) remaining cartilaginous (Fig. 9). In those specimens showing maximum ossification, the intermedium proximally wedges between the ulna and radius, and distally wedges between the centrale and ulnare (Fig. 9). The large radiale may represent a fusion of the radiale with element y, because no space for a possible element y is present in these specimens. The single large centrale is in direct contact with the radius, thus separating the radiale from contact with the intermedium. This pattern is also seen in

all other congeneric species, including *Batrachuperus yenyuanensis* (FMNH 49371), which is the only known species of the genus in which two centralia occur. In *B. londongensis*, the radiale is slightly smaller than the centrale, and articulates with the radius proximally, the basale commune distally and the centrale laterally. The basale commune is a large element, roughly triangular in shape. It is in articulation with the centrale proximally, and with metacarpal 1 and 2 distally. Distal carpal 3 is slightly smaller than distal carpal 4, and the two elements articulate with metacarpal III and IV, respectively.

There are four digits in the manus, the pattern seen in most salamanders. Digit 3 is the longest, having an extra phalange in comparison to the other digits. The phalangeal formula is 2-2-3-2, a generalized pattern for most salamanders (Shubin & Wake, 2003). The terminal phalange of each digit is covered with a cornified sheath, possibly an adaptive feature correlated to living in a mountain stream environment.

Pelvic girdle and hind limbs

The pelvis in *Batrachuperus londongensis* displays the usual pattern that occurs in most other salamanders: the paired ilia and ischia are ossified, whereas the pubis remains cartilaginous (but see below). In addition, the ypsiloid cartilage is present as in some but not all salamanders (see Hecht & Edwards, 1976a,b). The ilium is roughly club-shaped, with a slightly thickened and expanded ventral plate and a narrow dorsal blade. The ventral plate contributes to a large part of the acetabulum, and is ventrally in articulation with the ischium. The iliac blade is connected with the sacral rib by a ligament. The bone is set in a more or less vertical position, but the iliac blade is slightly inclined posteriorly.

The ischium is a large bony plate that is the main ventral element in the pelvis. The two ischial plates meet ventrally to form a symphysal hinge articulation along the midline. In ventral view, the ischium is anteriorly widened with a rounded border for attachment of the cartilaginous pubis (but see below), but projects laterally at the posteroventral border of the acetabulum. Immediately posterior to the acetabulum, the lateral border of the plate is deeply notched between the acetabulum and a large posterolateral process (ischial spine). The latter process is for attachment of the flexor of the tail, *M. ischio-caudalis* (Francis, 1934). The elongate ischial spine is significantly different from that in the type species *B. pinchonii*, in which the spine is rudimentary (see Zhang et al., 2009).

The pubis often remains cartilaginous, as observed in several specimens (CIB 14482, 14484, 14485, 14487, 14507); however, in several other specimens (CIB 65I0013/14380, 14381, 14504, 14509), the pubis is partly ossified, evidenced by the presence of a robust process anteroventral to the acetabulum. This interpretation is supported by the presence of an obturator foramen at the base of the process, which marks the border between the pubis and ischium (best shown in CIB 65I0013/14380, 14504). In addition, two of these specimens (CIB 14381, 14509) show that the fusion of the ossified part of pubis to the ischium is not yet completed; thus, in these two specimens the obturator foramen is still partly open anteromedially (Fig. 10). In them, the large ventral plate in the pelvis actually represents the ossification of the ischium and at least a part of the pubis, and can best be termed a pubio-ischium.

It is also interesting to note that many specimens including the holotype display a second pair of small foramina more posteriorly located at the base of the ischial spine (Fig. 10). In our knowledge, no published literature has figured or described this pair of foramina, but they are

indeed present in both neotenic and postmetamorphic individuals of *Batrachuperus londongensis*.



A Y-shaped ypsiloid cartilage is observed in cleared and stained specimens, but is not

shown in CT-scanned images. This cartilage has been shown to be correlated with the hydro-

static function of the lungs (Whipple, 1906); that is, the salamander can easily raise its head in

the water by elevating the ypsiloid cartilage, thereby compressing the lower abdomen and

forcing the air in the lungs forwards to the anterior end; conversely, the salamander is able to

depress its head by lowering the ypsiloid cartilage, returning the air to the posterior portion of the

lungs, enabling the animal to swim to deeper water. The ypsiloid cartilage is present in


Hynobiidae, Cryptobranchidae, Salamandridae, and Ambystomatidae, but absent in Proteidae,

Plethodontidae, Sirenidae, and Amphiumidae (Hecht & Edwards, 1976a,b).

The femur is a robust element roughly the same length as the humerus. As seen in the

holotype and several other specimens (CIB 65I0013/14380, 14381, 14504, 14507, 14509), the

strongly expanded proximal end bears a large bony condyle in articulation with the acetabulum

(Fig. 10). In four other specimens (CIB 14482, 14484, 14485, 14487), however, the humerus is 

capped with cartilage; thus, CT images of these specimens display a gap between the femur and

acetabulum. On the extensor side, the femur bears a longitudinal ridge, extending from the

proximal end to the fibular condyle; this ridge is for insertion of the M. pubo-ischio-femoralis

internus, a powerful extensor of the thigh (Francis, 1934). Posterior to this ridge and close to the


proximal end, a small tubercle marks the external trochanter, for insertion of the M. caudalis-


femoralis (Francis, 1934). On the flexor side, the robust femoral trochanter projects

ventromedially as a twig-like process, for insertion of the M. puboischiofemoralis externus

(Ashley-Ross, 1992). The trochanteric crest extends from the femoral trochanter distally along

908 the shaft to the tibial condyle. On the distal end, both the tibial and fibular condyles are well
 909 ossified for articulation with their corresponding elements. The tibial condyle is obviously much
 910 larger than that for the fibula. As described above for the proximal head, in some specimens
 911 (CIB 14482, 14484, 14485, 14487) the tibial and fibular condyles are poorly ossified, with
 912 slightly concave depressions as indicative of a cartilage-capped epiphysis.

 913 The **tibia and fibula** are similar in length, but the former element is the more robust.
 914 Proximally on its extensor aspect, the tibia bears a weakly developed tibial crest for a tendinous
 915 insertion of the M. extensor ilio-tibialis (Francis, 1934). Along the distal half of the tibia is a
 916 well-defined bony ridge facing the fibula; this medial ridge is probably for insertion of the M.
 917 extensor cruris tibialis (Ashley-Ross, 1992). At the proximal end of the medial ridge, a small but
 918 twig-like process is for a tendinous insertion of the M. pubo-ischio-tibialis (Francis, 1934). The
 919 lateral side of the fibula is straight but the medial side concave, with its distal end expanded
 920 medially to contact the tibia.

921 Maximum ossification of the mesopodium includes as many as nine tarsal elements (Fig.
 922 11). As observed in several specimens (CIB 65I0013/14380, 14381, 14485, 14509), the
 923 intermedium is a large element with its proximal process wedged between the tibia and fibula;
 924 the intermedium distally articulates with a single centrale. The fibulare is roughly the same size
 925 as the intermedium and is medially in extensive articulation with the latter. The tibiale is much
 926 smaller than the fibulare, but medially articulates with the centrale. Among distal elements,
 927 element y is more or less rounded, in articulation with the tibiale proximally and with a large
 928 basale commune laterally. Distal tarsal 3 and 4  are similar in size, and are both in contact with
 929 the centrale. **Distal tarsal 5** is obviously missing, in keeping with the loss of digit 5.
 930 Distolaterally, the postminimus is a small bone in contact with both the fibulare and metacarpal

IV. Comparison of different specimens with variable degrees of ossification indicates that the postminimus is probably the last tarsal element to be ossified (see below). According to Shubin & Wake (2003), a postminimus is present in *Batrachuperus* and several other hynobiids (*Liua*, *Ranodon*, *Salamandrella*, *Paradactylodon*), and also in the cryptobranchid *Andrias*.

Several other specimens show less extensive ossification in the mesopodium than those described above. As observed in four specimens (CIB 14482, 14482, 14484, 14487), all those elements ossified already show essentially the same arrangement pattern as described above, but have one or two of the preaxial elements (tibiale and element y) still unossified. In addition, in none of these specimens is the postminimus ossified. Comparison of these specimens with those described above indicates that element y ossifies before the tibiale, whereas the postminimus is ossified after the tibiale; thus, the postminimus is the last tarsal element to be ossified

ontogenetically.



As in all congeneric species, *Batrachuperus londongensis* displays a reduction of hind limb digits from five to four, with digit 5 missing. The phalangeal formula is 2-2-3-2, except for two specimens (CIB 14484, 14504) that show developmental abnormalities (see below). The terminal phalanges are covered with a cornified sheath as occurs commonly in other mountain stream salamanders, including the Middle Eastern stream salamander *Paradactylodon* (Kami, 1999).

As mentioned above, two specimens (CIB 14484, 14504) show developmental abnormalities in the hind limb. In CIB 14484, the right foot has four digits, but five in the left. In keeping with the presence of digit 5, a distal tarsal 5 is also present in the left foot but not in the right. The digital formula in this specimen is 2-2-2-2-2 in the right foot, and 2-2-3-2 in the left. The other specimen (CIB 14504) has only three digits in left foot, with digit 1 entirely

954 missing; but there are four digits in the right. The left foot has only six tarsal elements, whereas
 955 the right has ten, including two centralia. The six tarsals in the left may reflect abnormal fusion
 956 of several bones: possibly fusion of the intermedium with the centrale, and fusion of distal tarsals
 957 2+3. The fibulare is enlarged to be roughly the same size as the intermedium. Both left and
 958 right limbs have a small postminimus, indicative of this individual being a fully grown adult.
 959 The digital formula of this specimen is ?-2-3-2 for the left foot, and is 2-2-2-2 for the right.

960

961 **Discussion**

962 The Longdong Stream Salamander, *Batrachuperus londongensis*, is a rare hynobiid species that
 963 is of special interest because of a life-history that features facultative neoteny. In addition,
 964 undertaking an osteological study of this salamander is urgent, because of its rarity and current
 965 vulnerability to extinction (Jiang et al., 2016). From comparison with other species of the genus
 966 and other hynobiids, our study has revealed several osteological features that are diagnostic of *B.*
 967 *londongensis*, while several other features are shown to be of developmental, ecological, or
 968 phylogenetic significance. We provide a discussion of these results below.

969

970 **Osteological characterization of *Batrachuperus londongensis***

971 Previously, *Batrachuperus londongensis* had been diagnosed with reference only to external
 972 morphological characters and the number of chromosomes (Liu & Tian, 1978; Fei, Ye & Tian,
 973 1983; Fei et al., 2006). In supplementing the diagnosis of this species by inclusion of
 974 osteological features, our study shows that some of these diagnostic features are also
 975 phylogenetically significant in respect to both hynobiids and to the evolution of salamanders
 976 more generally. Osteologically, *Batrachuperus londongensis* shares with its congeneric species

the following derived characters: the maxilla is extremely short, posteriorly terminating at a level anterior to midlevel of the orbit; the lacrimal enters the border of the external naris anteriorly, but does not enter the orbital border posteriorly (except for *B. taibaiensis*); a nasal-maxillary contact is absent owing to intervention by the lacrimal; the otic process of the pterygoid has no bony contact with the parasphenoid (except for *B. yenyuanensis*); the ceratohyal is distally ossified; a single centrale (except for *B. yenyuanensis*) in the manus is in direct contact with the radius, preventing the radiale from contacting the intermedium; the number of digits is reduced from five to four in the pes (shared with *Salamandrella* and *Paradactylodon* as homoplasies); terminal phalanges are covered with a cornified sheath (shared with *Onychodactylus*, *Liua*, *Paradactylodon* as ecological homoplasies).

Batrachuperus londongensis is distinguished from *B. pinchonii* and all other congeneric species by a combination of the following characters: alary process of premaxilla barely contributing to border of anterodorsal fenestra (shared with *B. tibetanus*); suture between nasal and frontal located at the level of anterior border of orbit; vomers do not contact at the midline (unique); vomerine teeth four to eight in number, arranged in a nearly vertically oriented straight line; the ascending process of the palatoquadrate is ossified as a pillar between the parietal and the otic process of the pterygoid (shared with *B. tibetanus* and *B. taibaiensis*); radial loops stemming from basibranchial I do not cross one another (shared with *B. pinchonii*, *B. tibetanus*; unknown for other species); cartilaginous hypobranchial I and ceratobranchial I remain separate (fused in *B. pinchonii* and *B. tibetanus*); presacral vertebrae 18 in number; the scapular blade is extremely short, bearing a prominent posterodorsal process (unique); the ischial plate is penetrated by a small nerve foramen, and the ischial spine is clearly more elongated than in other species.

1000

1001 **Developmental features related to life-history differences**

1002 As stated above (see Introduction), *Batrachuperus londongensis* may represent the only living
1003 hynobiid that is facultatively neotenic, as both biphasic individuals and neotenes (“permanent
1004 larval producers” of Rose, 2003) are known for the species. Both neotenic and postmetamorphic
1005 individuals have been collected from the type locality, Longdong Stream, at an elevation of 1300
1006 m above sea level at Mt. Emei (Fei et al., 2006; Fei, Ye & Jiang, 2010).

1007 In terms of body size, neotenes tend to be larger than postmetamorphic individuals. The
1008 holotype CIB 65I0013/14380 (TL= 265 mm) is the largest individual known for the species, but
1009 still retains gill slits and a larval configuration of the hyobranchium (Fei et al., 2006). Because
1010 many relatively small specimens (TL= 162–241 mm) have completed metamorphosis, the
1011 presence of external gill slits and retention of a larval hyobranchium in large individuals cannot
1012 be logically interpreted as ontogenetic features always leading to metamorphosis in
1013 *Batrachuperus londongensis*. ~~On the other hand,~~ the holotype and several other large individuals
1014 display fully ossified limbs and a postminimus in the pes, thereby giving a clear indication that
1015 these are fully grown adults, in spite of their retention of some larval features.

1016 The most striking morphological difference between neotenic and postmetamorphic
1017 individuals is seen in the hyobranchium. As figured in Fei et al. (2006: fig. 69f, g), neotenes
1018 always display a more complex hyobranchium than do postmetamorphic individuals, in which
1019 ceratobranchial III–IV are entirely missing. ~~In regards,~~ median elements, the inverted “T-shaped”
1020 basibranchial II occurs in both postmetamorphic and neotenic forms, whereas the so-called “fork”-
1021 shaped pattern is seen only in some neotenes as a developmental feature. We provide a possible
1022 interpretation here: the “fork”-shaped pattern can be viewed as the initial larval pattern, with the

posterior branches subsequently absorbed at metamorphosis, whereas in neotenes the absorption process is prolonged or delayed. This interpretation is supported by evidence that large neotenic individuals, including the holotype CIB 65I0013/14380, ~~that~~ display the inverted “T”-shaped pattern, still have a remnant of the posterior processes, whereas slightly smaller and presumably younger adults show the “fork”-shaped pattern.

In respect to the laterally paired elements, both neotenic and postmetamorphic individuals show incomplete ossification of the ceratohyal, with large neotenes displaying more extensive ossification than smaller ones. This observation indicates that ossification of the ceratohyal terminates at metamorphosis, but continues ~~to take place~~ in neotenes. Hypobranchial I is partly ossified in large neotenes, but the element is missing in typical postmetamorphic forms (see below). ~~On the other hand,~~ ceratobranchial I is partly ossified only in neotenes. Evidently, then, ossification of the first branchial arch derivatives is terminated at metamorphosis, but is prolonged in neotenes. Ossification of hypobranchial II and ceratobranchial II is a common pattern in all hynobiids, whereas ceratobranchial III–IV are ~~only~~ retained in neotenic individuals, ~~but~~ are normally absent in postmetamorphic forms. CIB 14487 is a relatively small postmetamorphic adult, but it retains remnant part of ceratobranchial III bilaterally. Comparison of this specimen with those that show the typical postmetamorphic pattern of the hyobranchium indicates that resorption of larval arches can be prolonged until after metamorphosis is otherwise completed.

Partial ossification of ceratohyal in hynobiids

Comparison of *Batrachuperus londongensis* with congeneric species and other hynobiids suggests that partial ossification of the ceratohyal is a feature of phylogenetic significance.

Within *Batrachuperus*, a similar pattern of ossification of the ceratohyal occurs in *B. tibetanus* (FMNH 5901), *B. pinchonii* (Zhang et al., 2009: fig. 24), *B. karlschmidtii* (FMNH 49380), *B. yenyuanensis* (FMNH 49371), and *B. taibaiensis* (CIB 20040235). Xiong et al. (2013b: fig. 1E,H) illustrated *B. pinchonii* and *Liua shihi* as having the ceratohyal entirely cartilaginous, but characterized this structure in the description as partly ossified in these two species. Based on our own observations, we conclude that partial ossification of the ceratohyal occurs in all species of *Batrachuperus*.

~~Compared with other~~ hynobiids, partial ossification of the ceratohyal occurs in the monotypic *Pachyhynobius shangchengensis* and in *Ranodon sibiricus* (Fei & Ye, 1983; Fei et al., 2006; Xiong et al., 2013b: fig. 1G, however, shows no ossification in *R. sibiricus*), and in *Liua shihi* (Zhang, 1985; Fei et al., 2006; contra Xiong et al., 2013b: fig. 1, but mentioned as partly ossified in the description). In addition, our observation of a specimen of *Paradactylodon mustersi* (FMNH 211936) shows that it also displays a partly ossified ceratohyal. Another species, *Paradactylodon persicus* (MVZ 241494; AmphibiaTree, 2004) shows no ossification of the ceratohyal, but the specimen seems to be a young adult, as the nasals do not yet fully meet at the midline and a small parietal fontanelle is not yet completely closed. Ossification of the ceratohyal in four hynobiid genera (*Onychodactylus*, *Salamandrella*, *Pseudohynobius*, *Hynobius*) has yet to be recorded.

In the closely related clade Cryptobranchidae, the distal end of the ceratohyal is ossified in the North American hellbender *Cryptobranchus alleganiensis* (Elwood & Cundall, 1994: fig. 9; Rose, 2003: fig. 5), but not in the Chinese or Japanese giant salamander *Andrias* (Sato, 1943; Aoyama, 1930; Wu, 1982; Rose, 2003). Among ~~non-cryptobranchoid~~ salamanders, partial ossification of the ceratohyal is seen in some salamandrids (e.g., *Notophthalmus viridescens*) and

some dicamptodontids (e.g., *Dicamptodon ensatus*), in *Siren* and *Pseudobranchius*, and in *Proteus* but not in *Necturus* (see Rose, 2003 for citations). Clearly, the distribution of this character needs to be scrutinized in a cladistic analysis to understand its phylogenetic significance.

Ossification patterns of mesopodial elements and reduction of number of digits

Salamander limbs display variant structural patterns that provide significant information for addressing questions of morphological evolution in terms of ecological adaptation (Shubin & Wake, 2003). In this context, several limb features of *Batrachuperus londongensis*, including the arrangement of mesopodial elements and the reduction of the number of digits, are worth consideration in comparison with other congeneric species and other hynobiids as well.

Limb structures in hynobiid salamanders have been documented in the literature for several genera (*Onychodactylus*, *Batrachuperus*, *Salamandrella*, *Liua*, *Ranodon*, *Paradactylodon*), but remain largely unknown or poorly known for several others (*Hynobius*, *Pachyhynobius*, *Pseudohynobius*). *Batrachuperus* has been regarded as having two centralia (Shubin & Wake, 2003), but this interpretation was probably based on *B. yenyuanensis*, which indeed has two centralia; however, this study revealed that all other species of the genus, including the type species *B. pinchonii*, have a single centrale in both manus and pes. Although the single centrale is in direct contact with the radius in the forelimb, it does not contact the tibia in the hind limb. A direct contact of the centrale with the radius has been recognized as a peculiar feature in extant salamanders, as it also occurs in some temnospondyls (Shubin & Wake, 2003). Regardless, *B. yenyuanensis* is the only species within *Batrachuperus* that possesses two

centralia. Phylogenetic analysis based on molecular data has shown that *B. yenyuanensis* occupies a basal position in relation to other species of the genus (Chen et al., 2015); thus, the single centrale in these other species is likely to be a derived state acquired within *Batrachuperus*. Among other hynobiids, retention of two centralia is known for several taxa, including *Liua*, *Ranodon*, *Salamandrella*, and *Paradactylodon* (Shubin & Wake, 2003).

Comparison of specimens of *Batrachuperus* species reveals a delayed ossification of preaxial elements in both fore- and hind limbs. In the forelimb, fully grown adults of *B. londongensis* (e.g., holotype CIB 65I0013/14380, 14381, 14482, 14504) display a large radiale, which probably reflects fusion of the radiale with element y, whereas young adults (e.g., CIB 14484, 14485, 14487) show no ossification of the preaxial elements. Whether the radiale and element y are co-ossified or fused together needs to be verified by developmental evidence. In the hind limb, fully grown adults (e.g., CIB 65I0013/14380, 14381, 14504, 14507, 14509) clearly show that the tibiale and element y are ossified as separate elements, with several young adults (e.g., CIB 14482, 14484, 14485) showing that element y is ossified before the tibiale. Comparisons with other species of *Batrachuperus* and other hynobiids are needed to understand the ontogenetic and phylogenetic significance of these patterns.

According to Shubin & Wake (2003), a postminimus is present in *Batrachuperus* and several other genera of hynobiid salamanders (*Onychodactylus*, *Liua*, *Ranodon*, *Salamandrella*, *Paradactylodon*), and also the cryptobranchid genus *Andrias*. Comparison of specimens of congeneric species in this study concurs with Shubin and Wake (2003) on that congeneric species in *Batrachuperus* indeed have a postminimus in pes, and this is probably the last limb element to be ossified ontogenetically, as the postminimus is observed in fully grown adults but not in those young adults that have element y, or element y and tibiale ossified (see above). The

1115 postminimus is absent in *Hynobius*, *Pachyhynobius*, and *Pseudohynobius* (Shubin & Wake,
1116 2003). Although relevant information on presence/absence of this element is still sketchy for
1117 some hynobiid taxa, we interpret that possession of a postminimus as a plesiomorphic feature is
1118 widely distributed in the family Hyobiidae, whereas how many taxa at generic level share the
1119 loss of the element as a homology, or independent loss of this element need to be scrutinized in a
1120 thorough phylogenetic analysis.

1121 Finally, *Batrachuperus londongensis* displays limb patterns commonly seen in other
1122 mountain stream salamanders: The number of digits is reduced from five to four in hind limb,
1123 and terminal phalanges in both fingers and toes are covered with a cornified sheath. These
1124 features have been recognized as corresponding to ecological adaptations of the salamanders to
1125 higher altitude mountain stream environments (Fei & Ye, 1984). These limb features are not
1126 only seen in all other congeneric species, but also occur in other hynobiids (*Salamandrella*,
1127 *Paradactylodon*, and some species of *Hynobius*), which are also mountain stream dwellers
1128 (Reilly, 1983; Fei et al., 2006). However, several hynobiids (*Onychodactylus*, *Ranodon*, *Liua*)
1129 are also mountain stream dwellers, but none of these show reduction of digits from five to four in
1130 pes, and *Onychodactylus* is the only genus other than those mentioned above has developed
1131 claw-like terminal phalanges with a cornified sheath (Fei et al., 2006).

1132

1133 Conclusions

1134 Our study of the osteological anatomy of *Batrachuperus londongensis* has led to the following
1135 conclusions:

1136 1) *Batrachuperus londongensis* is diagnosed by a set of osteological features, including
1137 unique features: alary process of premaxilla is excluded from the border of the anterodorsal

fenestra; vomers lack medial contact; parasphenoid enters anteromedial fenestra; vomerine tooth row nearly vertical in position; presacral vertebrae 18 in number; scapular blade develops a distinct posterodorsal process.

2) *B. londongensis* is among the few hynobiids that display perichondral ossification of the ascending process of the palatoquadrate as a part of the suspensorium.

3) A stapedial foramen is unexpectedly present in some but not all specimens, an unusual feature that needs to be thoroughly investigated.

4) Neotenic individuals display a more complex structural pattern of the hyobranchium than postmetamorphic individuals, most notably the retention of ceratobranchial III and IV. Neotenes also show increased ossification of hyobranchial elements during aging, in contrast to loss of elements by resorption in metamorphic individuals.

5) *B. londongensis* has a single centrale in direct contact with the radius in the manus, but not with the corresponding element, the tibia, in the pes. In both fore- and hind limbs, delayed ossification of preaxial elements is a common pattern in both neotenes and postmetamorphic specimens.

6) *B. londongensis* retains element y and the postminimus in the pes as a plesiomorphic pattern in hynobiids. Phylogenetic significance of the retention or loss of these limb elements within Hynobiidae requires a thorough investigation.

Acknowledgements

We thank Alan Resetar (Field Museum of Natural History) for access to comparative specimens under his care, and Zhe-Xi Luo (University of Chicago) for use of the CT scanner in his laboratory. Professor RC Fox (University of Alberta) read and commented on the manuscript,

and Yu-long Li (Chengdu Institute of Biology, CAS) helped with CT scanning of some specimens. We also thank Neil Shubin (University of Chicago) for discussion on ossification patterns and evolution of the mesopodium in salamanders.

ADDITIONAL INFORMATION AND DECLARATIONS

Funding

This research was supported by the National Natural Science Foundation of China (NSFC 41672003) and National Key R & D Program of China (2017YFC0505202). The funders had no role in study design, data collection and analysis, decision to publish, preparation of the manuscript.

Grant Disclosures

The following grant information was disclosed by the authors: National Natural Science Foundation of China: NSFC 41672003; National Key R & D Program of China (2017YFC0505202).

Competing Interests

The authors declare there are no competing interests.

Author Contributions

- Jian-ping Jiang conceived and designed the experiments, analyzed the data, wrote the paper, reviewed drafts of the paper.
- Jia Jia conceived and performed the experiments, analyzed the data, prepared figure illustrations, reviewed drafts of the paper.
- Mei-hua Zhang performed the experiments, analyzed the data, reviewed drafts of the paper.

- Ke-Qin Gao conceived and designed the experiments, analyzed the data, prepared figure illustrations, wrote the paper, reviewed drafts of the paper.

Data Availability

The following information was supplied regarding data availability:

Detailed information on the specimens used in this study and CT scan images of the selected specimens have been supplied as Supplementary Files.

Supplemental Information

Supplemental information for this article can be found online at <http://dx.doi.org/....#supplemental-information>.

REFERENCES

- AmphibiaTree. 2004. *Batrachuperus persicus* (On-line), Digital Morphology. Accessed March 14, 2017 at http://digimorph.org/specimens/Batrachuperus_persicus/.
- AmphibiaTree. 2008. "*Ambystoma gracile*" (On-line), Digital Morphology. Accessed April 5, 2017 at http://digimorph.org/specimens/Ambystoma_gracile/head/.
- AmphibiaWeb. 2017. <<http://amphibiaweb.org>> University of California, Berkeley, CA, USA. (accessed 10 March 2017).
- Aoyama F.1930. Die Entwicklungsgeschichte des Kopfskelettes des *Cryptobranchus japonicus*. *Zeitschrift für Anatomie und Entwicklungsgeschichte* **93**:106–181.
- Ashley-Ross MA. 1992. The comparative myology of the thigh and crus in the salamanders *Ambystoma tigrinum* and *Dicamptodon tenebrosus*. *Journal of Morphology* **211**:147–163. DOI: 10.1002/jmor.1052110204.

- 1207 Boulenger GA. 1882. Catalogue of the Batrachia Gradientia Caudata s. and Batrachia Apoda in
1208 the Collection of the British Museum, 2nd edition, London: British Museum.
- 1209 Carroll RL, Holmes R. 1980. The skull and jaw musculature as guides to the ancestry of
1210 salamanders. *Zoological Journal of the Linnean Society* **68**:1–40. DOI: 10.1111/j.1096-
1211 3642.1980.tb01916.x
- 1212 Chen J, Gao KQ. 2009. Early Cretaceous hynobiid *Liaoxitriton zhongjiani* (Amphibia: Caudata)
1213 from Liaoning, China, and the monophyly of the Hynobiidae. *Journal of Vertebrate*
1214 *Paleontology* **29** (supplement to no. 3):76A. DOI: 10.1080/02724634.2009.10411818.
- 1215 Chen MY, Mao RL, Liang D, Kuro-o M, Zeng XM, Zhang P. 2015. A reinvestigation of
1216 phylogeny and divergence times of Hynobiidae (Amphibia, Caudata) based on 29 nuclear
1217 genes. *Molecular Phylogenetics and Evolution* **83**:1–6. DOI:
1218 10.1016/j.ympev.2014.10.010.
- 1219 Cloete SE. 1961. The cranial morphology of *Rhyacotriton olympicus olympicus* (Gauge). *Annals*
1220 *of the University of Stellenbosch* **36A**:113–145.
- 1221 Cope ED. 1859. On the primary divisions of the Salamandridae, with descriptions of two new
1222 species. *Proceedings of the Academy of Natural Sciences of Philadelphia* **11**:122–128.
- 1223 David A. 1872 (1871). Rapport adressé a MM. les Professeur-Administrateurs du Museum
1224 d’histoire naturelle. *Nouvelles Archives du Muséum d’Histoire Naturelle*. Paris **7**:75–100.
- 1225 De Beer GR. 1937. *The Development of the Vertebrate Skull*. Oxford: the Clarendon Press.
- 1226 Duellman WE, Trueb L. 1986. *Biology of Amphibians*. New York: McGraw-Hill Book
1227 Company.
- 1228 Duméril AMC. 1806. *Zoologie analytique, ou méthode naturelle de classification des animaux,*
1229 *rendue plus facile à l’aide de tableaux synoptiques*. Paris: Allais.

- 1230 Dunn ER. 1922. The sound-transmitting apparatus of salamanders and the phylogeny of the
1231 Caudata. *American Naturalist* **56**:418–427. DOI 10.1086/279882.
- 1232 Dunn ER. 1923. The salamanders of the family Hynobiidae. *Proceedings of the American*
1233 *Academy of Arts and Sciences* **58**:445–523. DOI: 10.2307/20026019.
- 1234 Edwards JL. 1976. Spinal nerves and their bearing on salamander phylogeny. *Journal of*
1235 *Morphology* **148**:305–328. DOI: 10.1002/jmor.1051480304.
- 1236 Elwood JRL, Cundall D. 1994. Morphology and behavior of the feeding apparatus in
1237 *Cryptobranchus alleganiensis* (Amphibia: Caudata). *Journal of Morphology* **220**: 47–70.
1238 DOI: 10.1002/jmor.1052200106.
- 1239 Estes R. 1981. *Encyclopedia of Paleoherpetology, Part 2: Gymnophiona, Caudata*. Stuttgart:
1240 Gustav Fischer Verlag.
- 1241 Fei L, Ye C. 1983. Systematic studies on Hynobiidae, including diagnosis of a new genus
1242 *Pseudohynobius* (Amphibia: Caudata). *Acta Herpetologica Sinica* **2**: 31–37. (in Chinese
1243 with English abstract).
- 1244 Fei L, Ye C. 1984. On the geographical-distribution, center of differentiation and phylogenetic-
1245 relationships of the different genera of Hynobiidae (Amphibia, Salamandriformes). *Acta*
1246 *Zoologica Sinica* **30**:385–392. (in Chinese with English abstract).
- 1247 Fei L, Ye C. 2001. *The Color Handbook of the Amphibians of Sichuan*. Chengdu, China: Sichuan
1248 Forestry Department, Sichuan Association of Wildlife Conservation, and Chengdu
1249 Institute of Biology.
- 1250 Fei L, Ye C. 2017. *Amphibians of China (Vol. I)*. Beijing: Science Press.

- 1251 Fei L, Ye C, Tian W. 1983. Systematic discussion on the genus *Batrachuperus* with description
1252 of a new species. *Acta Zootaxonomica Sinica* **8**:209–219. (in Chinese with English
1253 abstract).
- 1254 Fei L, Hu S, Ye C, Huang Y. 2006. *Fauna Sinica Amphibia volume 1*. Beijing: Science Press (in
1255 Chinese with English abstract).
- 1256 Fei L, Ye C, Jiang J. 2010. *Colored Atlas of Chinese Amphibians*. Chengdu: Sichuan Publishing
1257 Group.
- 1258 Fei L, Ye C, Jiang J. 2012. *Colored Atlas of Chinese Amphibians and Their Distributions*.
1259 Chengdu: Sichuan Publishing Group.
- 1260 Fox H. 1959. A study of the development of the head and pharynx of the larval urodele *Hynobius*
1261 and its bearing on the evolution of the vertebrate head. *Philosophical transactions of the*
1262 *Royal Society of London. Series B, Biological Sciences* **242**:151–204. URL:
1263 <http://www.jstor.org/stable/2992618>.
- 1264 Francis ETB. 1934. *The Anatomy of the Salamander*. Oxford: Clarendon Press.
- 1265 Frost DR. 2017. Amphibian Species of the World: an Online Reference. Version 6.0. (accessed 4
1266 March 2017). Electronic Database accessible at
1267 <http://research.amnh.org/herpetology/amphibia/index.html>. American Museum of Natural
1268 History, New York, USA.
- 1269 Fu J, Zeng X. 2008. How many species are in the genus *Batrachuperus*? A phylogeographical
1270 analysis of the stream salamanders (family Hynobiidae) from southwestern China.
1271 *Molecular Ecology* **17**(6):1469–1488. DOI: 10.1111/j.1365-294X.2007.03681.x.

- 1272 Fu J, Wang Y, Zeng X, Liu Z, Zheng Y. 2001. Genetic diversity of Eastern *Batrachuperus*
1273 (Caudata: Hynobiidae). *Copeia* **2001** (4):1100–1107. DOI: 10.1643/0045-
1274 8511(2001)001[1100:GDOEBC]2.0.CO;2.
- 1275 Fukuda Y. 1930. Die Veränderungen des Hyobranchialskeletts vom *Onychodactylus japonicus*
1276 bei der Metamorphose. *Folia Anatomica Japonica* **9**:47–72.
- 1277 Gao KQ, Shubin NH. 2001. Late Jurassic salamanders from northern China. *Nature* **410**:574–
1278 577. DOI: 10.1038/35069051.
- 1279 Gao KQ, Shubin NH. 2003. Earliest known crown-group salamanders. *Nature* **422**:424–428.
1280 DOI: 10.1038/nature01491.
- 1281 Gao KQ, Shubin HN. 2012. Late Jurassic salamandroid from western Liaoning, China.
1282 *Proceedings of the National Academy of Sciences of the United States of America*
1283 **109**:5767–5772. DOI: 10.1073/pnas.1009828109.
- 1284 Gao KQ, Chen J, Jia J. 2013. Taxonomic diversity, stratigraphic range, and exceptional
1285 preservation of Juro-Cretaceous salamanders from northern China. *Canadian Journal of*
1286 *Earth Sciences* **50**:255–267. DOI: 10.1139/e2012-039.
- 1287 Gaupp E. 1898. Ontogenese und Phylogenese des schalleitenden Apparates bei den Wirbeltieren.
1288 *Ergeb Anat Entwicklungsgeschichte herausg. v. Merkel. u. Bonnet, Bd. VIII*:990–1149.
- 1289 Gaupp E. 1911. Über den N. trochlearis der Urodelen und über die Austrittsstellen der
1290 Gehirnnerven aus dem Schädelraum im allgemeinen. *Anatomischer Anzeiger* **38**:401–444.
- 1291 Goodrich ES. 1930. *Studies on the Structure and Development of Vertebrates*. Chicago: The
1292 University of Chicago Press.

- 1293 Hecht MK, Edwards JL. 1976a. The determination of parallel or monophyletic relationships: the
1294 proteid salamanders- a test case. *The American Naturalist* **110**:653–677. DOI:
1295 10.1086/283096.
- 1296 Hecht MK, Edwards JL. 1976b. The methodology of phylogenetic inference above the species
1297 level. In: Hecht MK, Goody PC, Hecht BM, eds. *Major Patterns in Vertebrate Evolution*,
1298 New York and London: Plenum Press, 3–51.
- 1299 Inukai T. 1930-1932. Urodelenarten aus Nord Japan mit besonderer Berücksichtigung der
1300 Morphologie des Schädels. *Journal of the Faculty of Science, Hokkaido University*,
1301 *Series 6 Zoology* **1**:191–217.
- 1302 ICZN, 1999. International Code of Zoological Nomenclature. 4th edition, published by the
1303 international Trust for Zoological Nomenclature 1999.
- 1304 IUCN, 2016. *The IUCN Red List of Threatened Species*. Version 2016-2. www.iucnredlist.org.
1305 Downloaded on 30 October 2016.
- 1306 Ivachnenko M. 1978. Urodeles from the Triassic and Jurassic of Soviet Central Asia.
1307 *Paleontological Journal* **1978**:362–368.
- 1308 Jia J, Gao KQ. 2016a. A new hynobiid-like salamander (Amphibia, Urodela) from Inner
1309 Mongolia, China, provides a rare case study of developmental features in an Early
1310 Cretaceous fossil urodele. *PeerJ* **4**:e2499; DOI: 10.7717/peerj.2499.
- 1311 Jia J, Gao KQ. 2016b. A new basal salamandroid (Amphibia, Urodela) from the Late Jurassic of
1312 Qinglong, Hebei Province, China. *PLoS ONE* **11**:e0153834. DOI:
1313 10.1371/journal.pone.0153834.
- 1314 Jiang Z, Jiang J, Wang Y. et al. 2016. Red list of China’s vertebrates. *Biodiversity Science*
1315 **24**:500–553.

- 1316 Jömann N, Clemen G, Greven H. 2005. Notes on cranial ontogeny and delayed metamorphosis
1317 in the hynobiid salamander *Ranodon sibiricus* Kessler, 1866 (Urodela). *Annals of*
1318 *Anatomy* **187**:305–431. DOI: 10.1016/j.aanat.2005.02.010.
- 1319 Kami HG. 1999. Additional specimens of the Persian Mountain Salamander, *Batrachuperus*
1320 *persicus*, from Iran (Amphibia: Hynobiidae). *Zoology in the Middle East* **19**(1):37–42.
1321 DOI: 10.1080/09397140.1999.10637794. url:
1322 <http://dx.doi.org/10.1080/09397140.1999.10637794>
- 1323 Kingsbury BF, Reed HD. 1909. The columella auris in Amphibia. Second Contribution. *Journal*
1324 *of Morphology* **20**:549–628. DOI: 10.1002/jmor.1050200403.
- 1325 Larson, JHJ, Beneski JTJ, Miller BT. 1996. Structure and function of the hyolingual system in
1326 *Hynobius* and its bearing on the evolution of prey capture in terrestrial salamanders.
1327 *Journal of Morphology* **227**:235–248. DOI: 10.1002/(SICI)1097-
1328 4687(199602)227:2<235::AID-JMOR>3.0.CO;2-7.
- 1329 Lebedkina NS. 1964. The development of the dermal bones of the basement of the skull in
1330 Urodela (Hynobiidae). *Trudy Akademiia Nauk SSSR* **33**:75–172.
- 1331 Lebedkina NS. 2004. *Evolution of the Amphibian Skull*. Moscow: Pensoft Publishers.
- 1332 Litvinchuk SN, Borkin LJ. 2003. Variation in number of trunk vertebrae and in count of costal
1333 grooves in salamanders of the family Hynobiidae. *Contributions to Zoology* **72**: 195–209.
1334 url: <http://dpc.ubs.uva.nl/vol72/nr04/a01>
- 1335 Liu CC. 1950. Amphibians of Western China. *Chicago Natural History Museum Fieldiana*
1336 *Zoology Memoirs* **2**:1–400.

- 1337 Liu CC, Tian WS. 1978. In Liu, CC, Hu, SQ, Tian, WS. and Wu, GF. 1978: Four new amphibian
1338 species from Sichuan and Guangxi. *Materials for Herpetological Research Chengdu*
1339 **4**:18–19.
- 1340 Liu CC, Tian WS. 1983. In Fei L, Ye CY, Tian WS. 1983: Systematic discussion of the genus
1341 *Batrachuperus* with description of a new species (Salamandriiformes, Hynobiidae). *Acta*
1342 *Zootaxonomica Sinica* **8**:209–219. (in Chinese with English abstract)
- 1343 Monath T. 1965. The opercular apparatus of salamanders. *Journal of Morphology* **116**:149–170.
1344 DOI: 10.1002/jmor.1051160202.
- 1345 Morescalchi A. 1973. Amphibia. In: Chiarelli AB, Capanna E, eds. *Cytotaxonomy and*
1346 *Vertebrate Evolution*. New York and London: Academic Press, 233–348.
- 1347 Morescalchi A. 1975. Chromosome evolution in the caudate Amphibia. *Evolutionary Biology*
1348 **8**:339–387.
- 1349 Noble GK. 1931. *The Biology of the Amphibia*. New York and London: McGraw-Hill Book
1350 Company.
- 1351 Okajima K, Tsuaki T. 1921. Beiträge zur Morphologie des Skleralknorpels bei den Urodelen.
1352 *Zeitschrift für Anatomie und Entwicklungsgeschichte* **60**: 631–651.
- 1353 Olson EC. 1966. The middle ear—morphological types in amphibians and reptiles. *American*
1354 *Zoologist* **6**:399–419. DOI: <https://doi.org/10.1093/icb/6.3.399>.
- 1355 Reese AM. 1906. Anatomy of *Cryptobranchus allegheniensis*. *The American Naturalist* **40**:287–
1356 326. DOI: <https://doi.org/10.1086/278619>.
- 1357 Regel ED. 1970. Ascending process of the palatoquadratic cartilage in urodelans. *Doklady*
1358 *Akademii Nauk SSSR* **194**:509–512.
- 1359 Reilly SM. 1983. The biology of the high altitude salamander *Batrachuperus mustersi* from

- 1360 Afghanistan. *Journal of Herpetology* **17**:1–9. DOI: 10.2307/1563774.
- 1361 Reilly SM. 1987. Ontogeny of the hyobranchial apparatus in the salamanders *Ambystoma*
1362 *talpoideum* (Ambystomatidae) and *Notophthalmus viridescens* (Salamandridae): the
1363 ecological morphology of two neotenic strategies. *Journal of Morphology* **191**:205–214.
1364 DOI: 10.1002/jmor.1051910210.
- 1365 Reilly SM, Altig R. 1996. Cranial ontogeny in *Siren intermedia* (Caudata: Sirenidae):
1366 paedomorphic, metamorphic, and novel patterns of heterochrony. *Copeia* **1996**:29–41.
1367 DOI: 10.2307/1446939.
- 1368 Rose CS. 2003. The developmental morphology of salamander skulls. In: Heatwole H, Davies
1369 M, eds. *Amphibian Biology. Volume 5: Osteology*. Chipping Norton NSW: Surrey Beatty
1370 & Sons, 1684–1781.
- 1371 Sasaki M. 1924. On a Japanese salamander, in Lake Kutarush, which propagates like the axolotl.
1372 *Journal of the College of Agriculture, Hokkaido Imperial University* **15**:1–36.
- 1373 Sato I. 1943. *A Monograph of the Tailed Batrachians of Japan*. Osaka: Nippon Shuppan-sha.
- 1374 Sessions SK. 2008. Evolutionary cytogenetics in salamanders. *Chromosome Research* **16**:183–
1375 201. DOI:10.1007/s10577-007-1205-3.
- 1376 Schmalhausen II. 1958. Nasolacrimal duct and septomaxillare of Urodela. *Zoologicheskii*
1377 *Zhurnal* **37**:570–583.
- 1378 Schmalhausen II. 1968. *The Origin of Terrestrial Vertebrates*. New York: Academic Press.
- 1379 Scopoli JA. 1777. *Introductio ad historiam naturalem, sistens genera lapidum, plantarum et*
1380 *animalium hactenus detecta, characteribus essentialibus donata, in tribus divisa, subinde*
1381 *ad leges naturae*. Prague: Apud Wolfgangum Gerle.

- 1382 Shubin NH, Wake DB. 2003. Morphological variation, development, and evolution of the limb
- 1383 skeleton of salamanders. In: Heatwole H, Davies M, eds. *Amphibian Biology. Volume 5:*
- 1384 *Osteology*. New South Wales: Surrey Beatty and Sons, 1782–1808.
- 1385 Smirnov SV, Vassilieva AB. 2002a. Skeletal and dental ontogeny in the long-tailed clawed
- 1386 salamander, *Onychodactylus fischeri* (Urodela: Hynobiidae). *Russian Journal of*
- 1387 *Herpetology* **9**:21–32. URL: <http://rjh.folium.ru/index.php/rjh/article/view/590>.
- 1388 Smirnov SV, Vassilieva AB. 2002b. The bony skull of the Siberian salamander *Salamandrella*
- 1389 *keyserlingii* (Amphibia: Urodela: Hynobiidae) and the role of thyroid hormones in its
- 1390 development. *Doklady Biological Sciences* **385**:387–389. DOI:
- 1391 0.1023/A:1019985523014.
- 1392 Song M, Zeng X, Wu G, Liu Z, Fu J. 2001. A new species of *Batrachuperus* from northwestern
- 1393 China. *Asiatic Herpetological Research* **9**:6–8. DOI: 10.5962/bhl.part.15559.
- 1394 Sparreboom M. 2014. *Salamanders of the Old World*. Zeist: KNNV Publishing.
- 1395 Suzuki T. 1932. Development of the brain, nervous system, and cranial skeleton in amphibians.
- 1396 I. Development of the skull in *Onychodactylus japonicus*. *Kaibogaku Zassi (Acta*
- 1397 *Anatomica Japonica)* **5**:685–719.
- 1398 Trueb L. 1993. Patterns of cranial diversity among the Lissamphibia. In: Hanken J, Hall BK, eds.
- 1399 *The Skull, Volume 2: Patterns of Structural and Systematic Diversity*. Chicago: The
- 1400 University of Chicago Press, 255–343.
- 1401 Trueb L, Cloutier R. 1991. A phylogenetic investigation into the inter- and intrarelationships of
- 1402 the Lissamphibia (Amphibia: Temnospondyli). In: Schultze HP, Trueb L, eds. *Origins of*
- 1403 *the Higher Groups of Tetrapods: Controversy and Consensus*. Ithaca and London:
- 1404 Cornell University Press, 223–231.

- 1405 Vassilieva AB, Poyarkov NA, Iizuka K. 2013. Peculiarities [sic] of bony skeleton development in
1406 Asian clawed salamanders (*Onychodactylus*, *Hynobiidae*) related to embryonization.
1407 *Biology Bulletin* **40**:1–11. 589–599. DOI: 10.1134/S1062359013070078.
- 1408 Vassilieva AB, Lai JS, Yang SF, Chang YH, Poyarkov NA. Jr. 2015. Development of the bony
1409 skeleton in the Taiwan salamander, *Hynobius formosanus* Maki, 1922 (Caudata:
1410 *Hynobiidae*): heterochronies and reductions. *Vertebrate Zoology* **65**:117–130.
- 1411 Wake DB. 2001. "*Dicamptodon ensatus*" (On-line), Digital Morphology. Accessed April 5, 2017
1412 at http://digimorph.org/specimens/Dicamptodon_ensatus/.
- 1413 Worthington RD, Wake DB. 1971. Larval morphology and ontogeny of the ambystomatid
1414 salamander, *Rhyacotriton olympicus*. *American Midland Naturalist* **85**:349–365. DOI: 27
1415 10.2307/2423762.
- 1416 Wu C. 1982. External and skeletal anatomy of *Meglobatrachus davidianus*. *Journal of Zoology*
1417 **17**:11–16. (in Chinese)
- 1418 Wu G, Xie F. 2004. *Batrachuperus londongensis*. The IUCN Red List of Threatened Species
1419 2004: e.T59084A11867916.
1420 <http://dx.doi.org/10.2305/IUCN.UK.2004.RLTS.T59084A11867916.en>. Downloaded on
1421 01 January 2017.
- 1422 Xiong JL, Yu P, Zhang JL, Zhu WW, Sun P. 2013a. Vertebral column characteristics of
1423 *Batrachuperus pinchonii*, and discussion on the division of the vertebral column in
1424 Urodela. *Chinese Journal of Zoology* **48**:451–456. (in Chinese with English abstract).
- 1425 Xiong JL, Sun P, Zhang JL, Liu XY. 2013b. A comparative study of the hyobranchial apparatus
1426 in *Hynobiidae* (Amphibia: Urodela). *Zoology* **116**:99–105. DOI:
1427 10.1016/j.zool.2012.10.004.

1428 Zhang F. 1985. On anatomy of the skeletal system of *Liua shihi* (Liu) (Amphibia: Hynobiidae).
 1429 *Acta Herpetologica Sinica* **4**:17–24. (in Chinese with English abstract)

1430 Zhang H, Liu S, Zhao Y, Yang Q. 2009. Skeletal system of *Batrachuperus pinchonii*. *Sichuan*
 1431 *Journal of Zoology* **28**:412–416. (in Chinese with English abstract)

1432 Zhang P, Chen YQ, Zhou H, Liu Y-F, Wang L, Papenfuss TJ, Wake DB, Qu L-H. 2006.
 1433 Phylogeny, evolution, and biogeography of Asiatic salamanders (Hynobiidae).
 1434 *Proceedings of the National Academy of Sciences of the United States of America*
 1435 **103**:7360–7365. DOI: 10.1073/pnas.0602325103.

1436 Zheng Y, Peng R, Kuro-o M, Zeng X. 2011. Exploring patterns and extent of bias in estimating
 1437 divergence time from mitochondrial DNA sequence data in a particular lineage: a case
 1438 study of salamanders (Order Caudata). *Molecular Biology and Evolution* **28**:2521–2535.
 1439 DOI: 10.1093/molbev/msr072.

1440

1441

Figure Captions

Figure 1. Photographs of ethanol-preserved specimens of *Batrachuperus londongensis* in dorsal view: (A) holotype CIB 65I0013/14380; (B) referred specimen CIB 14381; (C) referred specimen CIB 14504. All topotypic specimens were collected from the type locality Longdong Stream, Mt. Emei, Sichuan Province, China.

Figure 2. Skull roof of *Batrachuperus londongensis*: (A) holotype CIB CIB65I0013/14380; (B) CIB 14481 (B); (C) CIB 14482. Note CIB 14482 in (C) displaying incomplete resorption of palatine.

Figure 3. Lateral view of the skull of *Batrachuperus londongensis*: (A) CIB CIB65I0013/14380; (B) CIB 14481; (C) CIB 14482. All images with squamosal and quadrate removed to expose the otic capsule. Note the unusual perichondral ossification of the ascending process of palatoquadrate as a pillar between the parietal and pterygoid anterior to the prootic.

Figure 4. Palatal view of the skull of *Batrachuperus londongensis*: (A) holotype CIB CIB65I0013/14380; (B) CIB 14481; (C) CIB 14482. Note that the two vomers have no midline contact behind the anteromedial fenestra; note also delayed resorption of palatine in CIB 14482 (C).

Figure 5. Mandible of *Batrachuperus londongensis*: right mandible of CIB 14482 in medial (A) and lateral (B) views; mandibular arch of CIB 14482 in dorsal (C) and ventral (D) views.

1465

1466 Figure 6. Hyobranchial apparatus of *Batrachuperus londongensis*: (A) CIB 14499, showing a
1467 neotenic pattern with extra ceratobranchial III and IV; (B) CIB 14504, showing a
1468 postmetamorphic pattern with ceratobranchial III and IV entirely lost by resorption.

1469

1470 Figure 7. Holotype skeleton of *Batrachuperus londongensis* (CIB65I0013/14380): CT rendered
1471 reconstruction of whole body of the holotype skeleton in dorsal (A) and ventral (B) views.

1472

1473 Figure 8. Pectoral girdle and upper arm of *Batrachuperus londongensis*: CIB65I0013/14380, left
1474 scapulocoracoid in lateral (A) and lateroventral (B) views; left scapulocoracoid of CIB 14381 in
1475 lateral (C) and lateroventral (D) views; left scapulocoracoid of CIB 14504 in lateral (E) and
1476 lateroventral (F) views; left humerus of CIB65I0013/14380 in dorsal (G) and ventral (H) views;
1477 right humerus of CIB 14381 in dorsal (I) and ventral (J) views; left humerus of CIB 14504 in
1478 dorsal (K) and ventral (L) views. Note unusual ossification of normally cartilaginous parts of
1479 procoracoid and coracoid in the holotype (A, B) and CIB 14504 (E, F).

1480

1481 Figure 9. Forearm of *Batrachuperus londongensis*: (A) CIB 14381; (B) CIB 14484; (C) CIB
1482 14487; (D) CIB 14507. All images display left forearm in dorsal view and not to scale; note
1483 presence of direct contact of the centrale with radius as an unusual feature in urodeles.

1484

1485 Figure 10. Pelvis and femur of *Batrachuperus londongensis*: Pelvis of CIB 65I0013/14380 in
1486 right lateral (A) and ventral (B) views; pelvis of CIB 14381 in right lateral (C) and ventral (D)
1487 views; pelvis of CIB 14482 in right lateral (E) and ventral (F) views; pelvis of CIB 14487 in

1488 right lateral (G) and ventral (H) views; left femur of CIB 65I0013/14380 in dorsal (I) and ventral
 1489 (J) views; left femur of CIB 14381 in dorsal (K) and ventral (L) views; left femur of CIB 14482
 1490 in dorsal (M) and ventral (N) views; left femur of CIB 14487 in dorsal (O) and ventral (P) views.

1491

1492 Figure 11. Lower hind limb of *Batrachuperus londongensis*: (A) left lower hind limb of
 1493 CIB65I0013/14380; (B) left lower hind limb of CIB 14381; (C) left lower hind limb of CIB
 1494 14482; (D) left lower hind limb of CIB 14487. All in dorsal view and not to scale.

1495

1496

1497

1498

1499

1500

1501

Figure 1

Photographs of ethanol-preserved specimens of *Batrachuperus londongensis* in dorsal view

Figure 1. Photographs of ethanol-preserved specimens of *Batrachuperus londongensis* in dorsal view: (A) holotype CIB 6510013/14380; (B) referred specimen CIB 14381; (C) referred specimen CIB 14504. All topotypic specimens were collected from the type locality Longdong Stream, Mt. Emei, Sichuan Province, China.

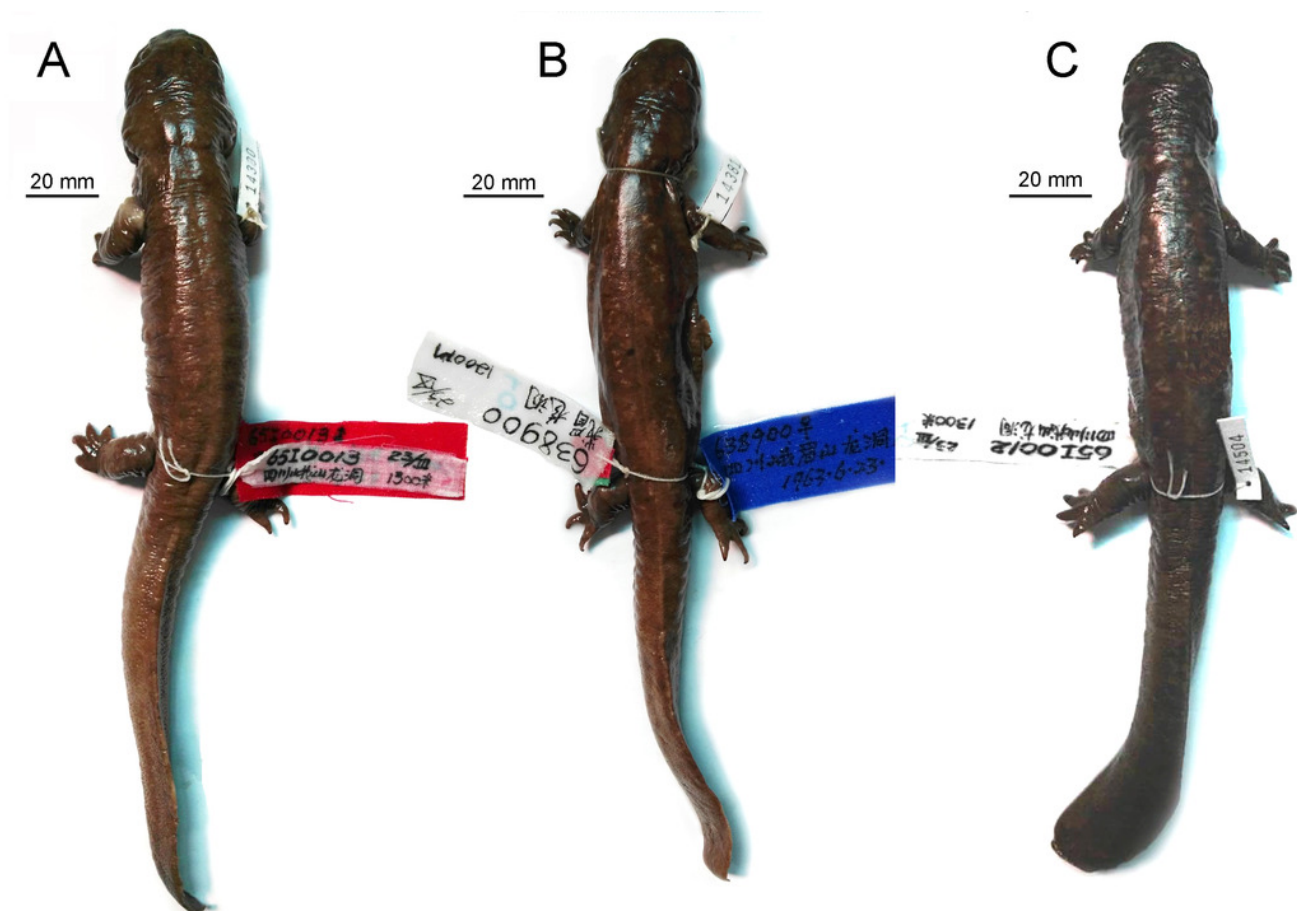


Figure 2

Skull roof of *Batrachuperus londongensis*

Figure 2. Skull roof of *Batrachuperus londongensis*: (A) holotype CIB CIB65I0013/14380; (B) CIB 14481 (B); (C) CIB 14482. Note CIB 14482 in (C) displaying incomplete resorption of palatine.

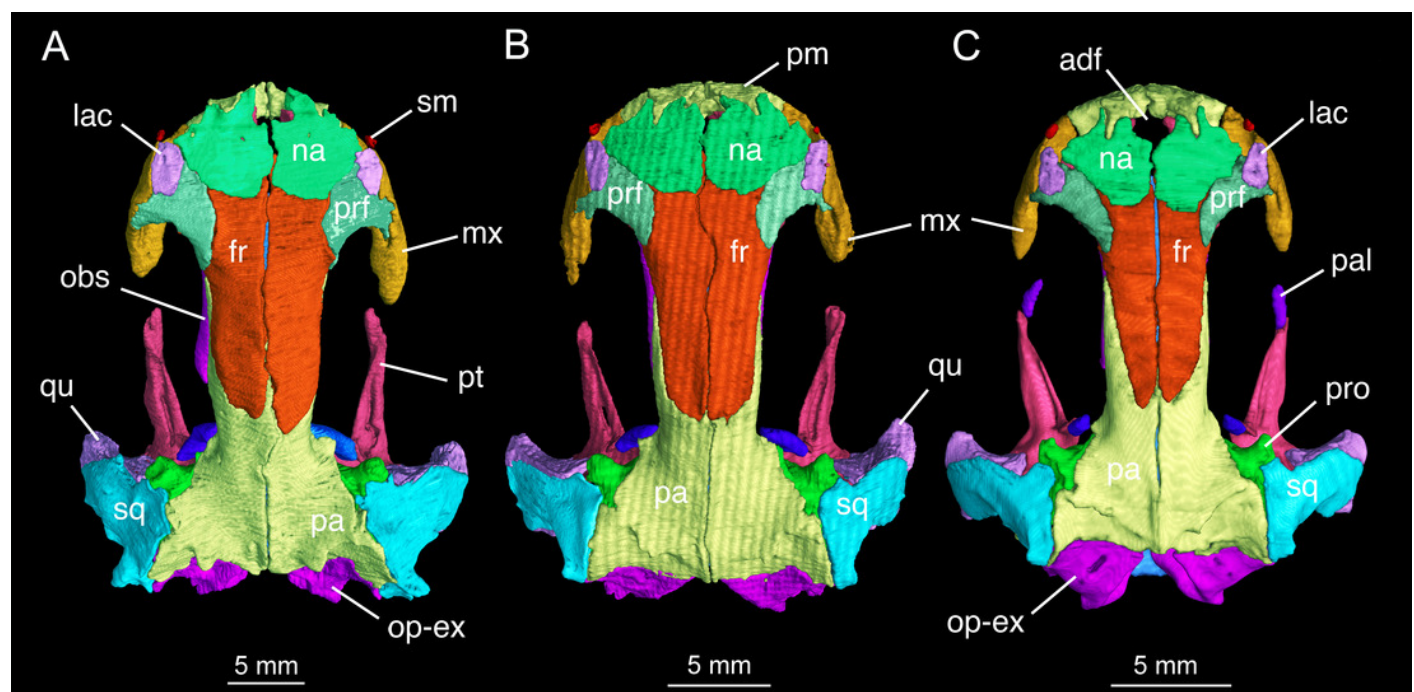


Figure 3

Lateral view of the skull of *Batrachuperus londongensis*

Figure 3. Lateral view of the skull of *Batrachuperus londongensis*: (A) CIB CIB65I0013/14380; (B) CIB 14481; (C) CIB 14482. All images with squamosal and quadrate removed to expose the otic capsule. Note the unusual perichondral ossification of the ascending process of palatoquadrate as a pillar between the parietal and pterygoid anterior to the prootic.

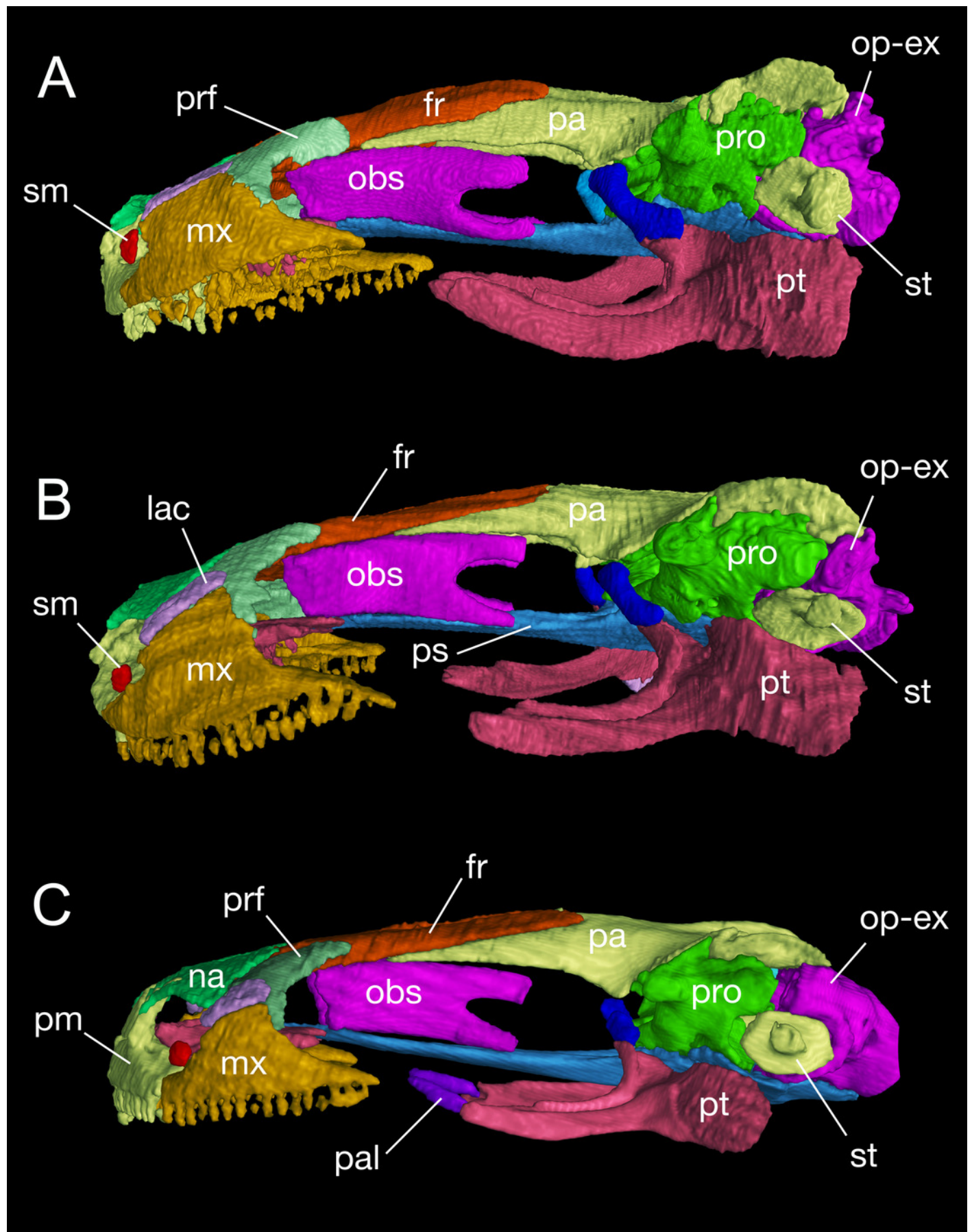


Figure 4

Palatal view of the skull of *Batrachuperus londongensis*

Figure 4. Palatal view of the skull of *Batrachuperus londongensis*: (A) holotype CIB CIB65I0013/14380; (B) CIB 14481; (C) CIB 14482. Note that the two vomers have no midline contact behind the anteromedial fenestra; note also delayed resorption of palatine in CIB 14482 (C).

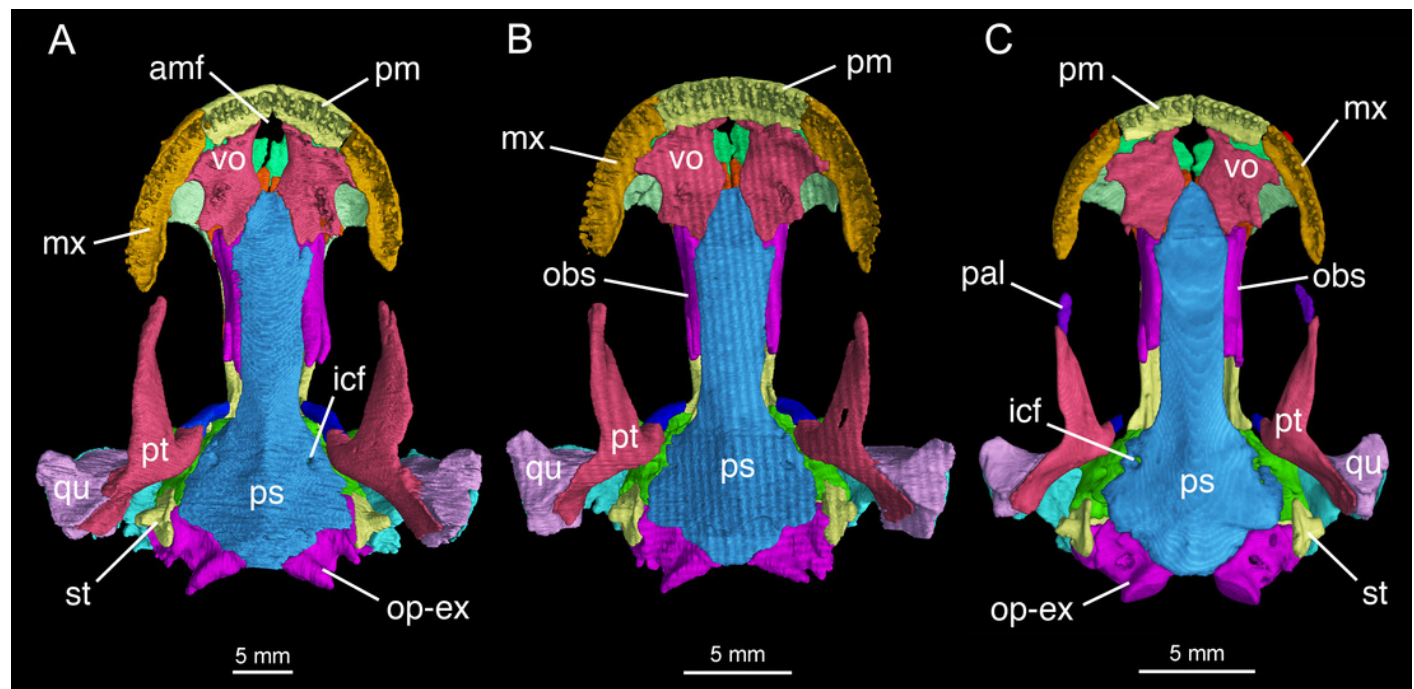


Figure 5

Mandible of *Batrachuperus londongensis*

Figure 5. Mandible of *Batrachuperus londongensis*: right mandible of CIB 14482 in medial (A) and lateral (B) views; mandibular arch of CIB 14482 in dorsal (C) and ventral (D) views.

**Note: Auto Gamma Correction was used for the image. This only affects the reviewing manuscript. See original source image if needed for review.*

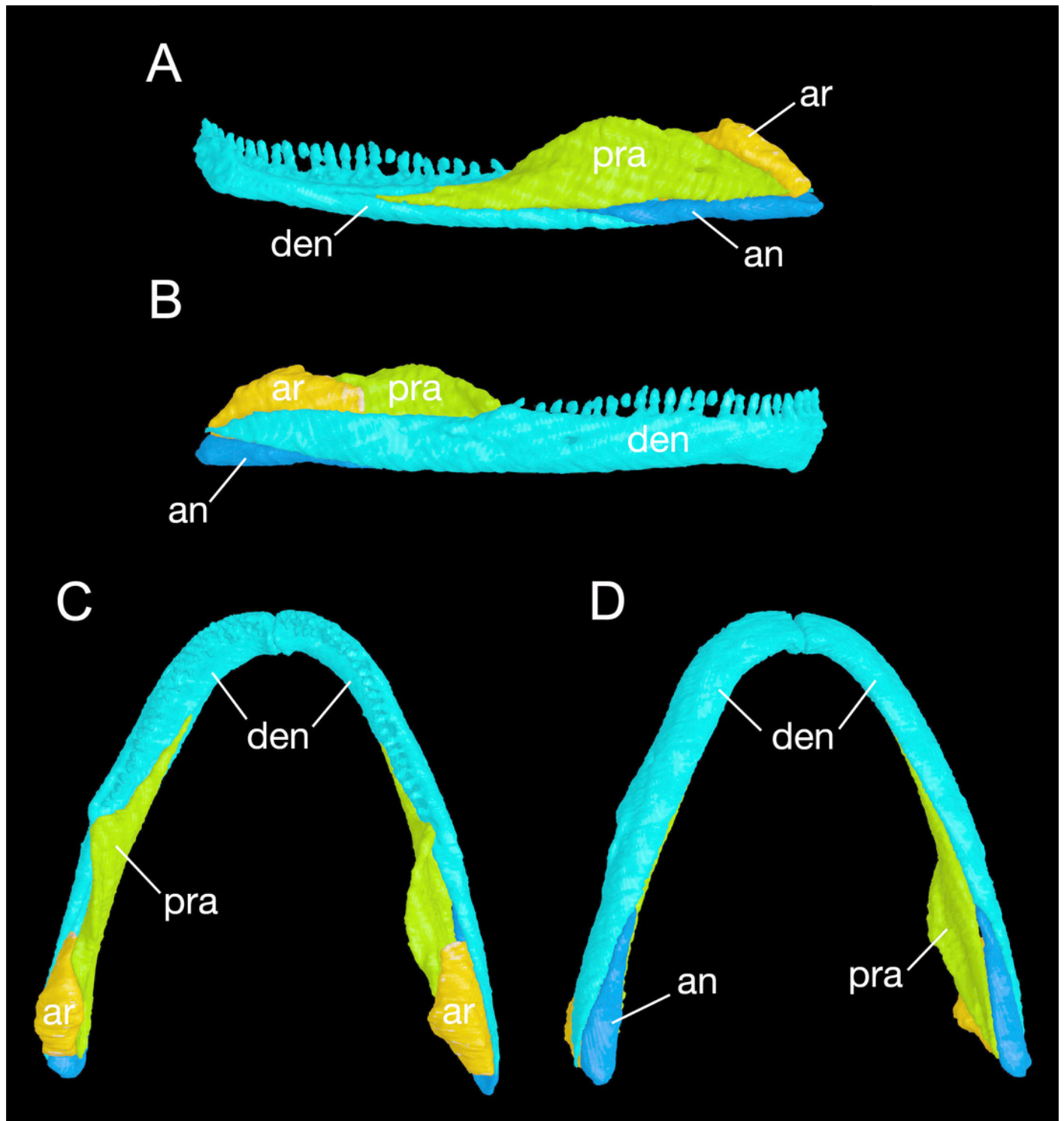


Figure 6

Hyobranchial apparatus of [i]Batrachuperus londongensis[i]

Figure 6. Hyobranchial apparatus of *Batrachuperus londongensis*: (A) CIB 14499, showing a neotenic pattern with extra ceratobranchial III and IV; (B) CIB 14504, showing a postmetamorphic pattern with ceratobranchial III and IV entirely lost by resorption.

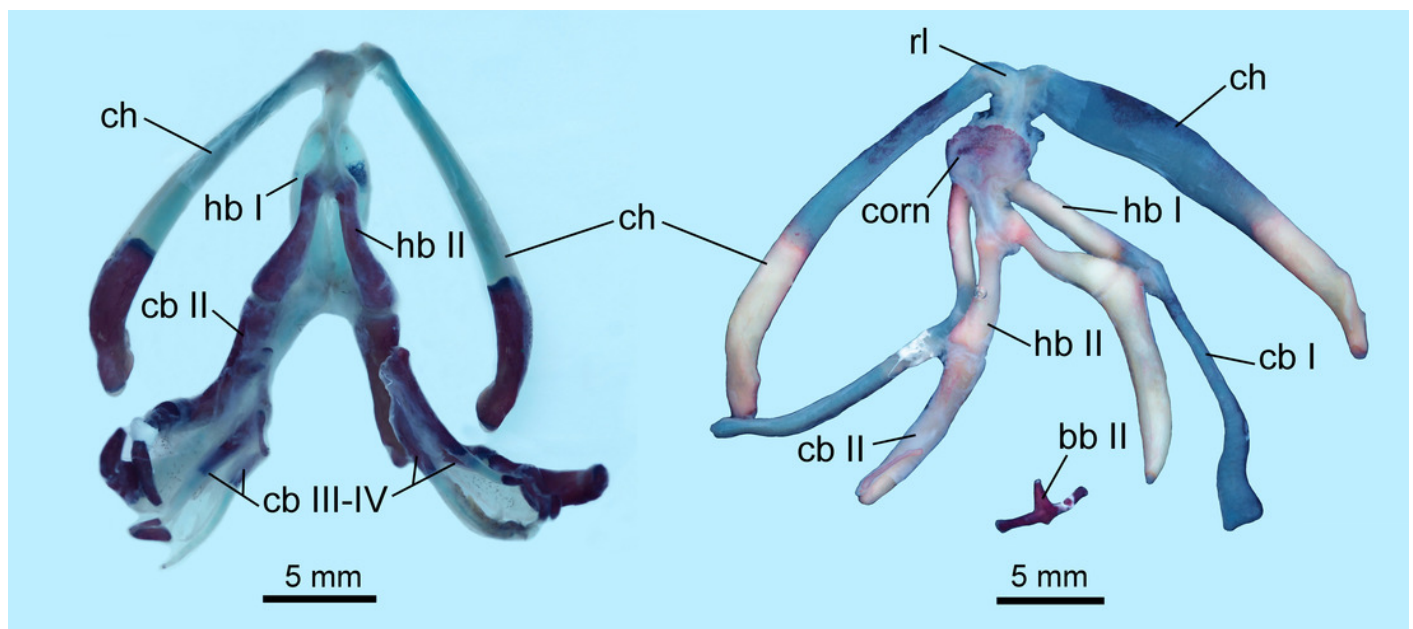


Figure 7

Holotype skeleton of *Batrachuperus londongensis* (CIB65I0013/14380)

Figure 7. Holotype skeleton of *Batrachuperus londongensis* (CIB65I0013/14380): CT rendered reconstruction of whole body of the holotype skeleton in dorsal (A) and ventral (B) views.

**Note: Auto Gamma Correction was used for the image. This only affects the reviewing manuscript. See original source image if needed for review.*

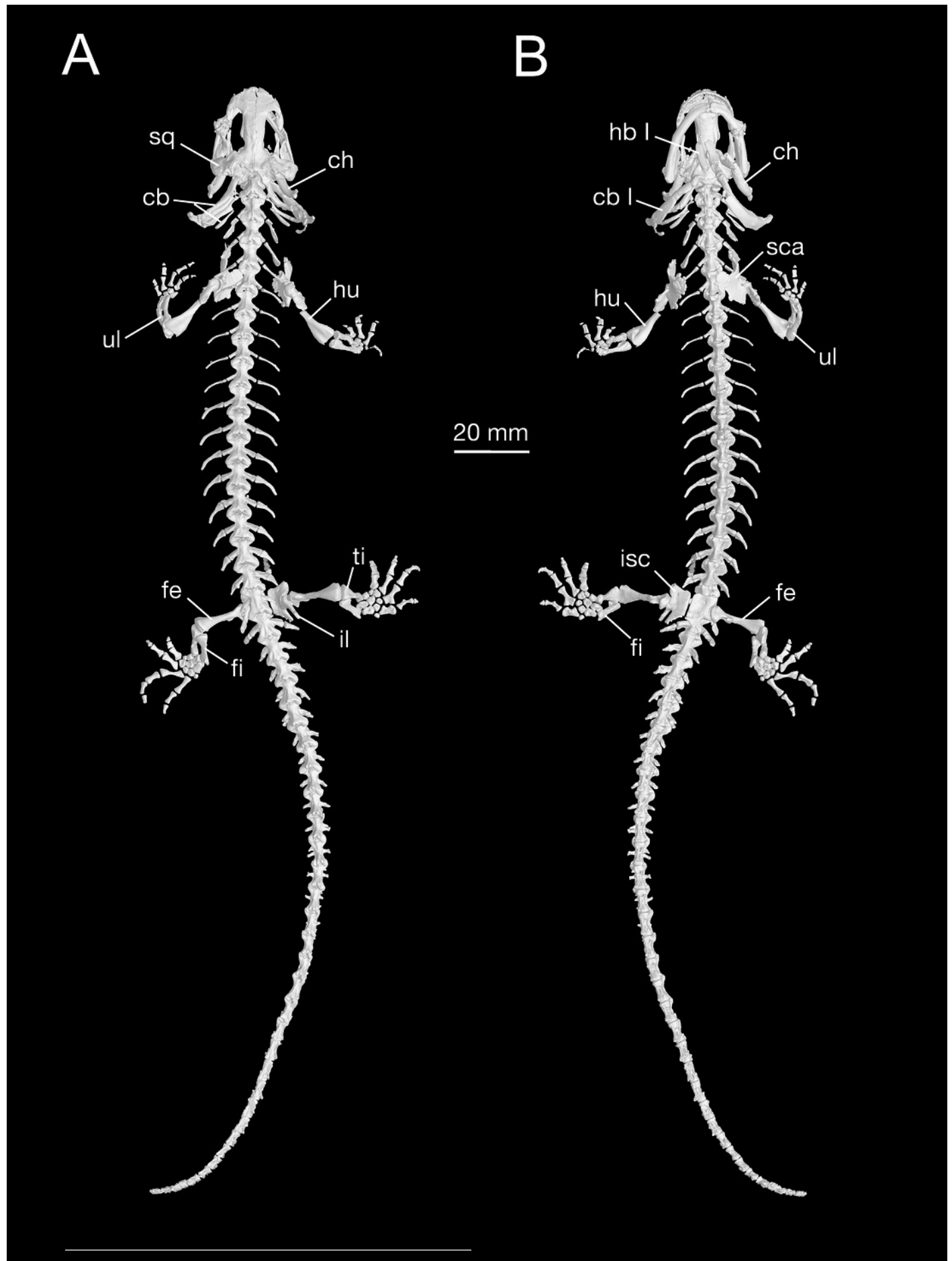


Figure 8

Pectoral girdle and upper arm of *Batrachuperus londongensis*

Figure 8. Pectoral girdle and upper arm of *Batrachuperus londongensis*: CIB65I0013/14380, left scapulocoracoid in lateral (A) and lateroventral (B) views; left scapulocoracoid of CIB 14381 in lateral (C) and lateroventral (D) views; left scapulocoracoid of CIB 14504 in lateral (E) and lateroventral (F) views; left humerus of CIB65I0013/14380 in dorsal (G) and ventral (H) views; right humerus of CIB 14381 in dorsal (I) and ventral (J) views; left humerus of CIB 14504 in dorsal (K) and ventral (L) views. Note unusual ossification of normally cartilaginous parts of procoracoid and coracoid in the holotype (A, B) and CIB 14504 (E, F).

**Note: Auto Gamma Correction was used for the image. This only affects the reviewing manuscript. See original source image if needed for review.*

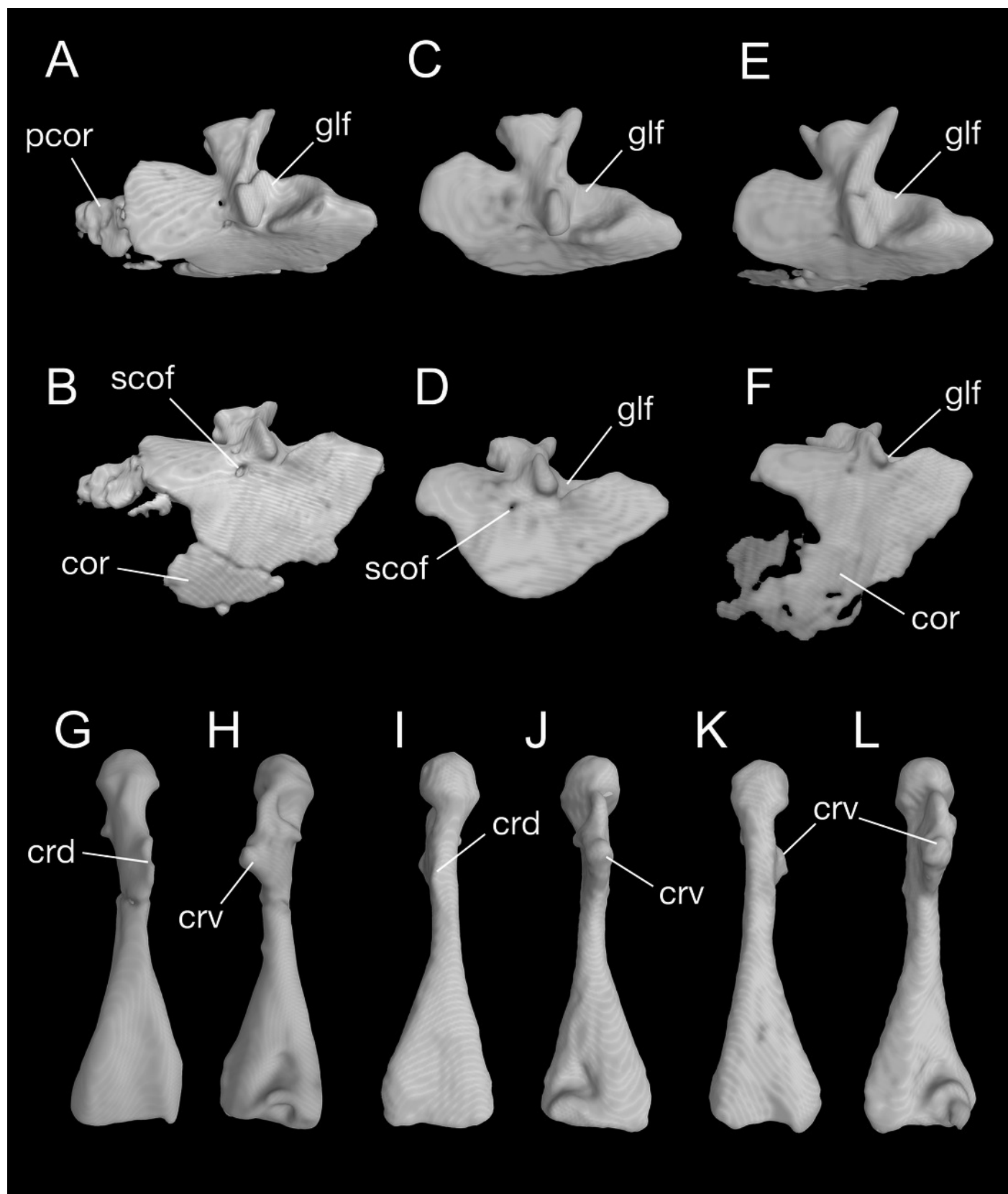


Figure 9

Forearm of *Batrachuperus londongensis*

Figure 9. Forearm of *Batrachuperus londongensis*: (A) CIB 14381; (B) CIB 14484; (C) CIB 14487; (D) CIB 14507. All images display left forearm in dorsal view and not to scale; note presence of direct contact of the centrale with radius as an unusual feature in urodeles.

**Note: Auto Gamma Correction was used for the image. This only affects the reviewing manuscript. See original source image if needed for review.*

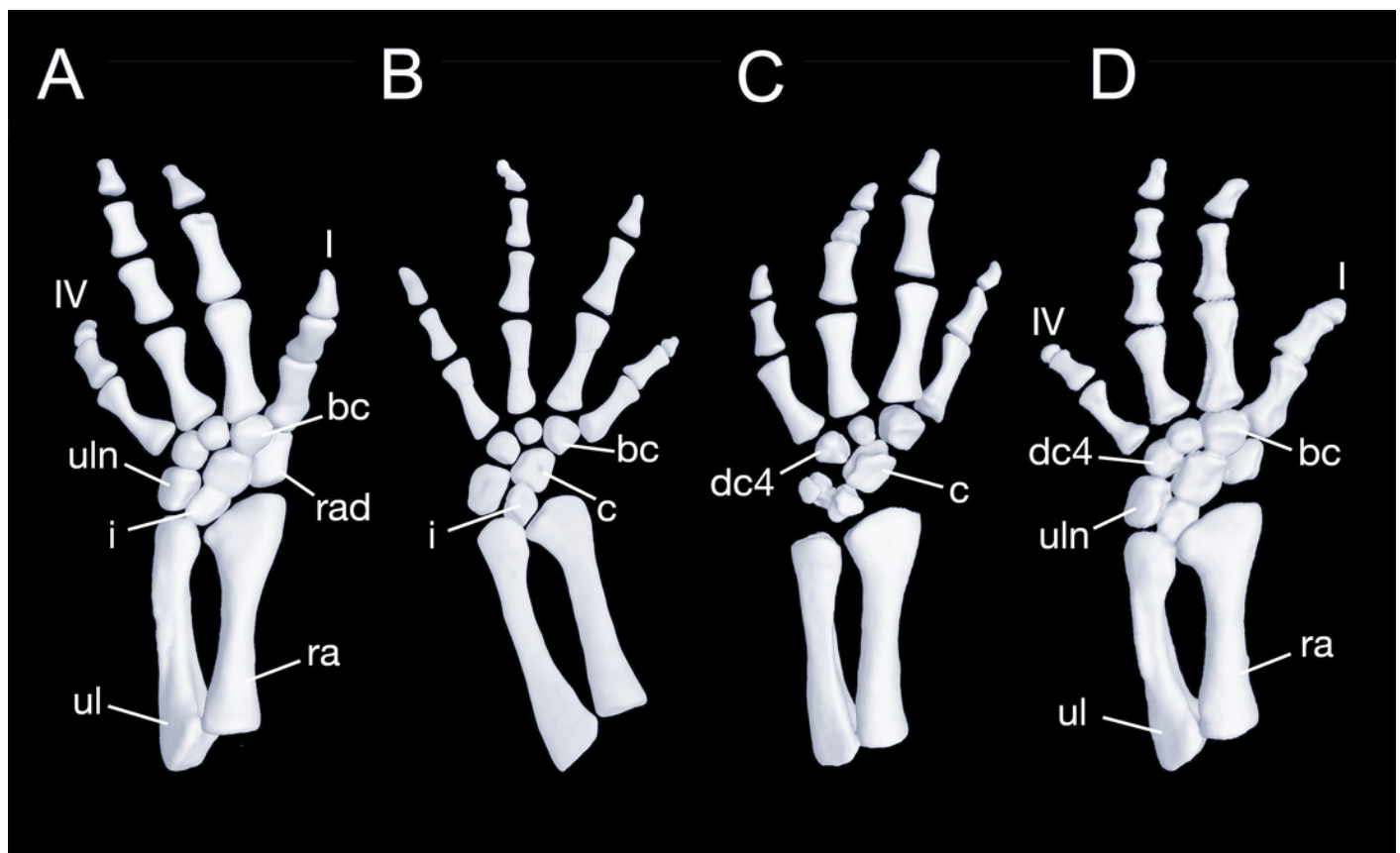


Figure 10

Pelvis and femur of *Batrachuperus londongensis*

Figure 10. Pelvis and femur of *Batrachuperus londongensis*: Pelvis of CIB 65I0013/14380 in right lateral (A) and ventral (B) views; pelvis of CIB 14381 in right lateral (C) and ventral (D) views; pelvis of CIB 14482 in right lateral (E) and ventral (F) views; pelvis of CIB 14487 in right lateral (G) and ventral (H) views; left femur of CIB 65I0013/14380 in dorsal (I) and ventral (J) views; left femur of CIB 14381 in dorsal (K) and ventral (L) views; left femur of CIB 14482 in dorsal (M) and ventral (N) views; left femur of CIB 14487 in dorsal (O) and ventral (P) views.

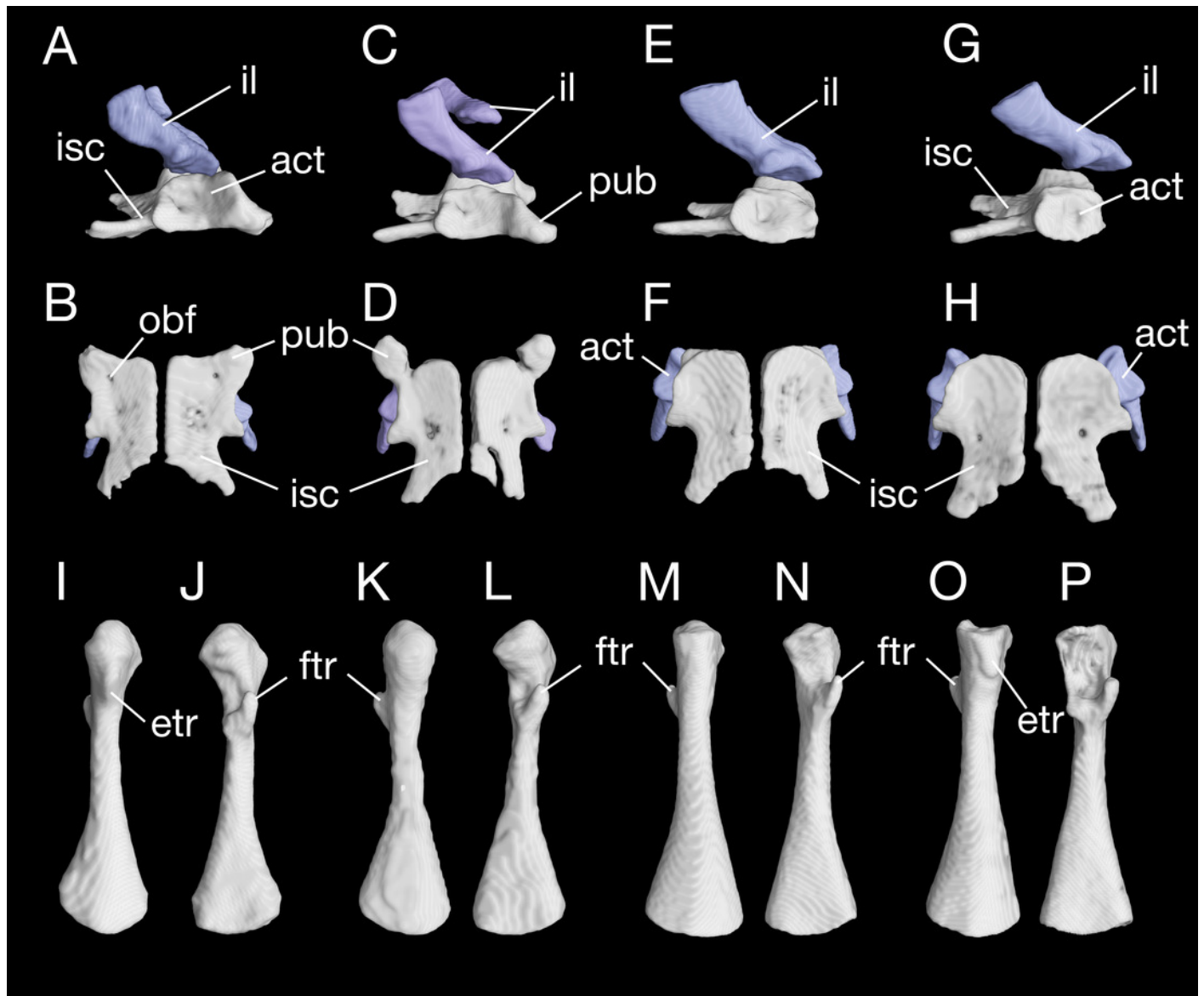


Figure 11

Lower hind limb of *Batrachuperus londongensis*

Figure 11. Lower hind limb of *Batrachuperus londongensis*: (A) left lower hind limb of CIB65I0013/14380; (B) left lower hind limb of CIB 14381; (C) left lower hind limb of CIB 14482; (D) left lower hind limb of CIB 14487. All in dorsal view and not to scale.

**Note: Auto Gamma Correction was used for the image. This only affects the reviewing manuscript. See original source image if needed for review.*

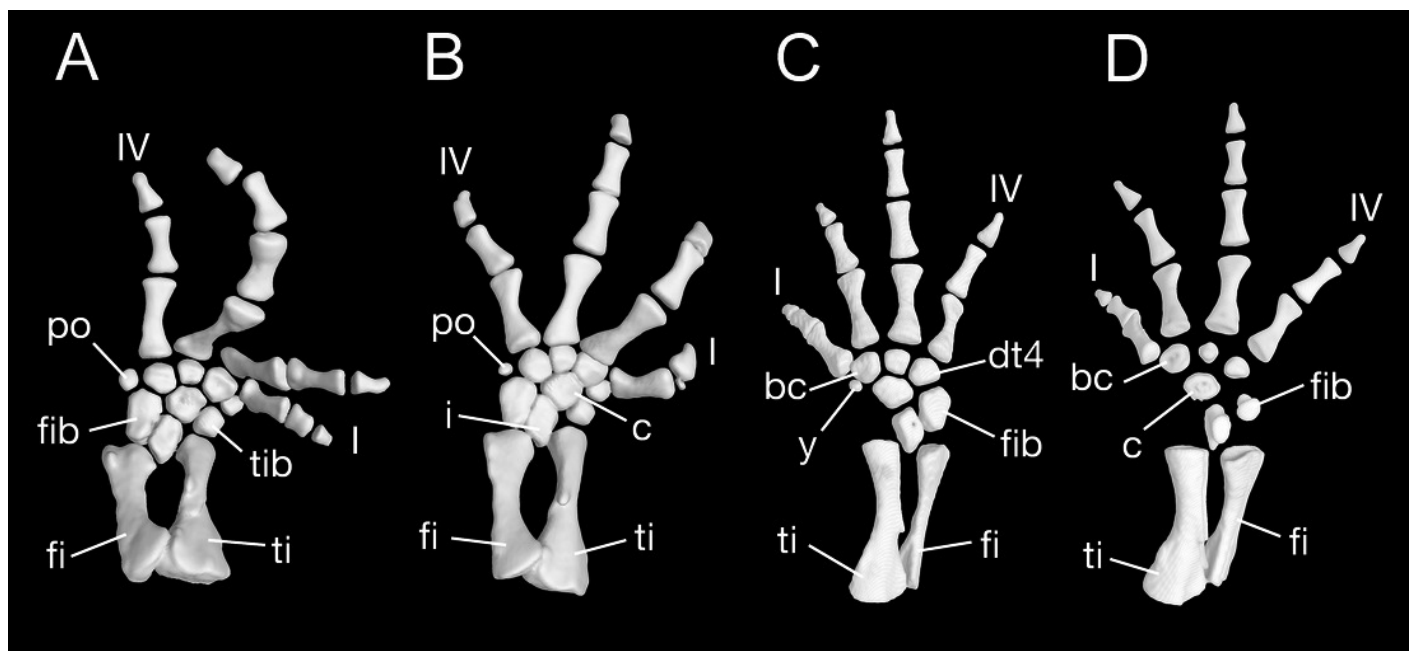


Table 1(on next page)

Measurements of specimens used in this study

Table 1. Measurements of specimens used in this study.

Table 1. Measurements of specimens used in this study

(Measurements in mm)

Catalogue Number	Field Number	Male/ Female	External Gill Slits	Total Length	Snout-Pelvic Length	Skull Length	Skull Width
CIB14504	65I0012	♀	absent	220.15	117.51	26.96	21.28
CIB14507	620593	♂	absent	225.35	120.32	34.08	25.69
CIB14509	638866	♀	absent	219.99	113.15	28.19	23.08
CIB14500	川 I00202	juven	absent	110.07	60.24	16.84	12.82
CIB14380	65I0013	♂	present	265.00	129.00	27.50	23.80
CIB14381	638900	♀	present	221.94	121.00	22.70	20.00
CIB 14482	99I0511	♀	present	178.28	98.10	25.94	17.38
CIB 14484	99I 0517	♂	present	189.05	97.93	26.73	18.35
CIB 14485	99I0520	♀	present	179.39	93.92	25.35	17.77
CIB 14487	99I0513	♂	absent	164.09	89.27	24.38	17.51
CIB 14499	川 I00196	♀	present	214.76	116.96	27.85	21.31